Geotechnical and Geological Engineering, 1997, **15** 47–85

Design of tabular excavations in foliated rock: an integrated numerical modelling approach

E. EBERHARDT*, D. STEAD†, M. J. REEVES* and C. CONNORS‡

*Department of Geological Sciences, University of Saskatchewan, Saskatoon, Saskatchewan, S7N 0W0, Canada
†Camborne Schools of Mines, University of Exeter, Redruth, Cornwall TR15 3SE, UK and
‡Hudson Bay Mining and Smelting Co. Limited., Flin Flon, Manitoba, Canada

Received 26 April 1996
Accepted 2 December 1996

Summary

This paper presents a rock mechanics design methodology applicable to steeply dipping orebodies typical of many underground hardrock mines. The first stage in the design process is the characterization of the rock mass using both *in situ* and laboratory data. The effects of anisotropy on rock mass behaviour are discussed with reference to laboratory and field observations. The second stage involves the use of a number of selected numerical modelling techniques to investigate ground response in the near-field rock mass surrounding the mining excavations. This study shows that the use of several numerical methods in conjunction, allowing for the advantages of each method to be maximized, provides a more comprehensive analysis of the different facets of stope design. This approach differs from those in the literature which seek to compare the different numerical methods in order to select just one method best suited for a problem. The design methodology employed emphasizes the importance of developing an understanding of ground deformation mechanisms as opposed to predicting absolute behaviour.

Keywords: Numerical modelling, mine design, tabular stopes, anisotropy

Introduction

Ore recovery from underground mining involves developing excavations to gain access to the mineralized zone (development openings), extracting the ore from the surrounding host rock (stopes), and transporting the material to the surface (permanent openings). The stoping operation forms the core of the mining process, requiring that the rock mass stability, both within the orebody and in the rock adjacent to the orebody, be controlled to ensure efficient and economical ore recovery. To provide this control, different stoping methods have been designed and used to extract the ore. Each method produces varied degrees and magnitudes of displacement in both the near- and far-field domains. One of the more common stoping methods used is the open stoping method. Pakalnis *et al*. (1987) report that approximately 51% of all ore production by underground metal mines in

Canada is derived directly from open stoping operations and the need for more cost-efficient mineral production will only serve to increase this.

Open stope mining involves opening a large excavation to allow for the extraction of ore. Opening these large excavations is accompanied by a redistribution of the *in situ* stress field and an increase in strain energy stored in the form of stress concentrations around the opening. The stope must remain open until all the ore is extracted under a specified minimal acceptable dilution criterion. Support for the free-standing stope walls is provided through the intact strength of the orebody and host rock, and by the pillars that separate the open stope from previously developed openings. In addition, cable bolting techniques and the use of backfill provides extra support and better ground control around the stope. Any design methodology must account for all of these factors in order to estimate the potential for ground instability, and recommend suitable mining strategies.

Geomechanical design methods are often used to study the effects that a large opening has on the local stress field and the stability of the stope walls. The primary goal of these methods is to assess the rock mass stability by analysing the effects that an excavation will have on the local stress field and whether the integrity of the rock mass will be compromised. Instability of the rock mass can result in increased dilution and unsafe ground conditions. Brady and Brown (1993) note that this enables a predictive analysis of the rock response to different stope and pillar layouts, as well as various extraction and sequencing strategies. Routine design techniques include analytical, empirical and numerical modelling methods. A study was undertaken to evaluate a variety of these techniques in order to provide an overall design rationale which would integrate the advantages of each method. A case study involving a sill pillar failure in the Trout Lake mine of the Hudson Bay Mining and Smelting Co., Ltd was used as part of this evaluation.

Case history background

The Trout Lake Cu–Zn sulphide deposit was discovered in 1976, 5 km northeast of Flin Flon, Manitoba (Fig. 1). The deposit lies within the Paleoproterozoic age Amisk volcanic strata of the Flin Flon Greenstone Belt and comprises both massive and disseminated sulphides. The presence of an extensive alteration zone underlying each of the sulphide lenses typifies a metamorphosed volcanogenic massive sulphide (VMS) ore deposit as defined by Franklin *et al.* (1981).

Production at the mine began in 1981 under a joint venture involving Hudson Bay Mining and Smelting (HBMS), Granges Exploration and Manitoba Mineral Resources, with mining occurring in two main ore zones, ‘north’ and ‘south’. Initial mining was carried out using the cut-and-fill method; as mining depth increased, a greater proportion was produced via open stope mining. Present production is concentrated in the ‘north’ zone; the case study discussed in this paper involves the failure of a stope (referred to as the #4 lens) in this zone.

The orebody consists of a series of en-echelon concordant massive sulphide lenses, each underlain by an altered zone of chloritized quartz–phyric fragmental rhyolite (locally called chlorite schist). Ko (1986) describes the massive sulphide ore as generally occurring

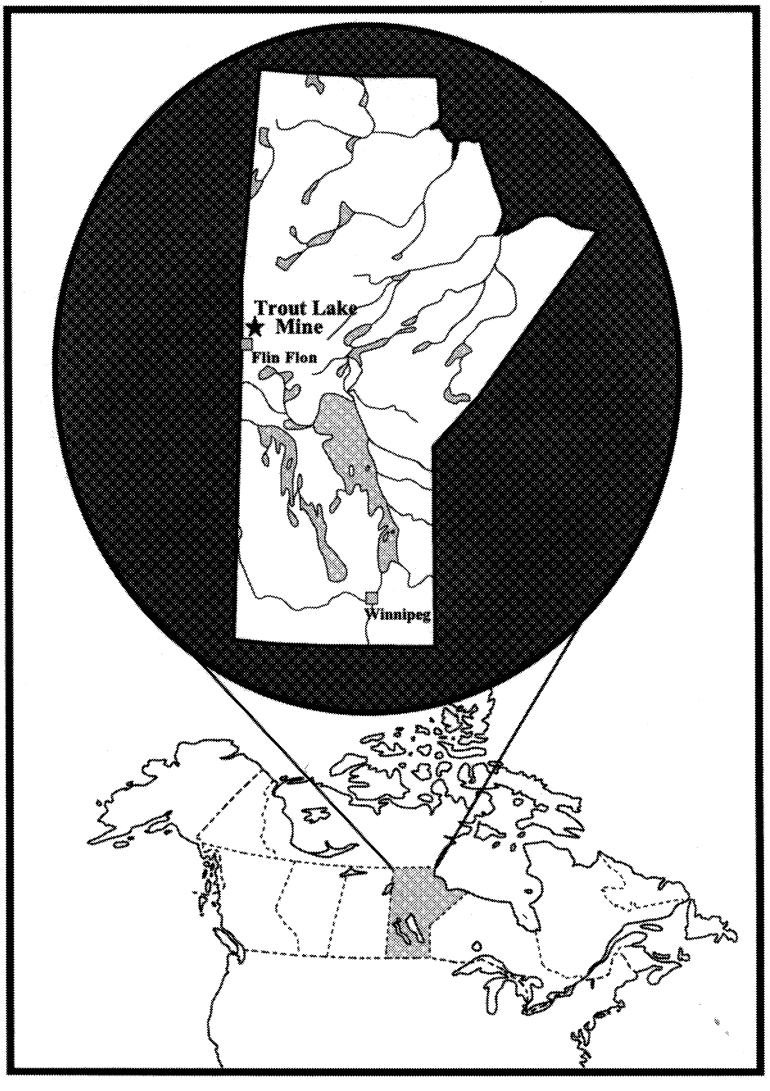

Fig. 1. Location of the Trout Lake mine

directly above the altered zone with disseminated sulphide ore appearing in the altered zone. Both are hosted by a sericitized quartz–phyric fragmental rhyolite (locally called quartz porphyry). The orebody, which is parallel to the stratigraphy, has a sharp contact with the fragmental quartz porphyry hangingwall and a diffuse contact with the chlorite schist footwall (Fig. 2). When the structure of the mine is examined, it can be seen that the orebody has been sliced into several lenses through shearing, with each slice being separated by narrow widths of moderately schistose and altered wall-rock. These lenses have been displaced for some distance both laterally and vertically. The geology of the #4 lens is consistent with the general geology of the mine.

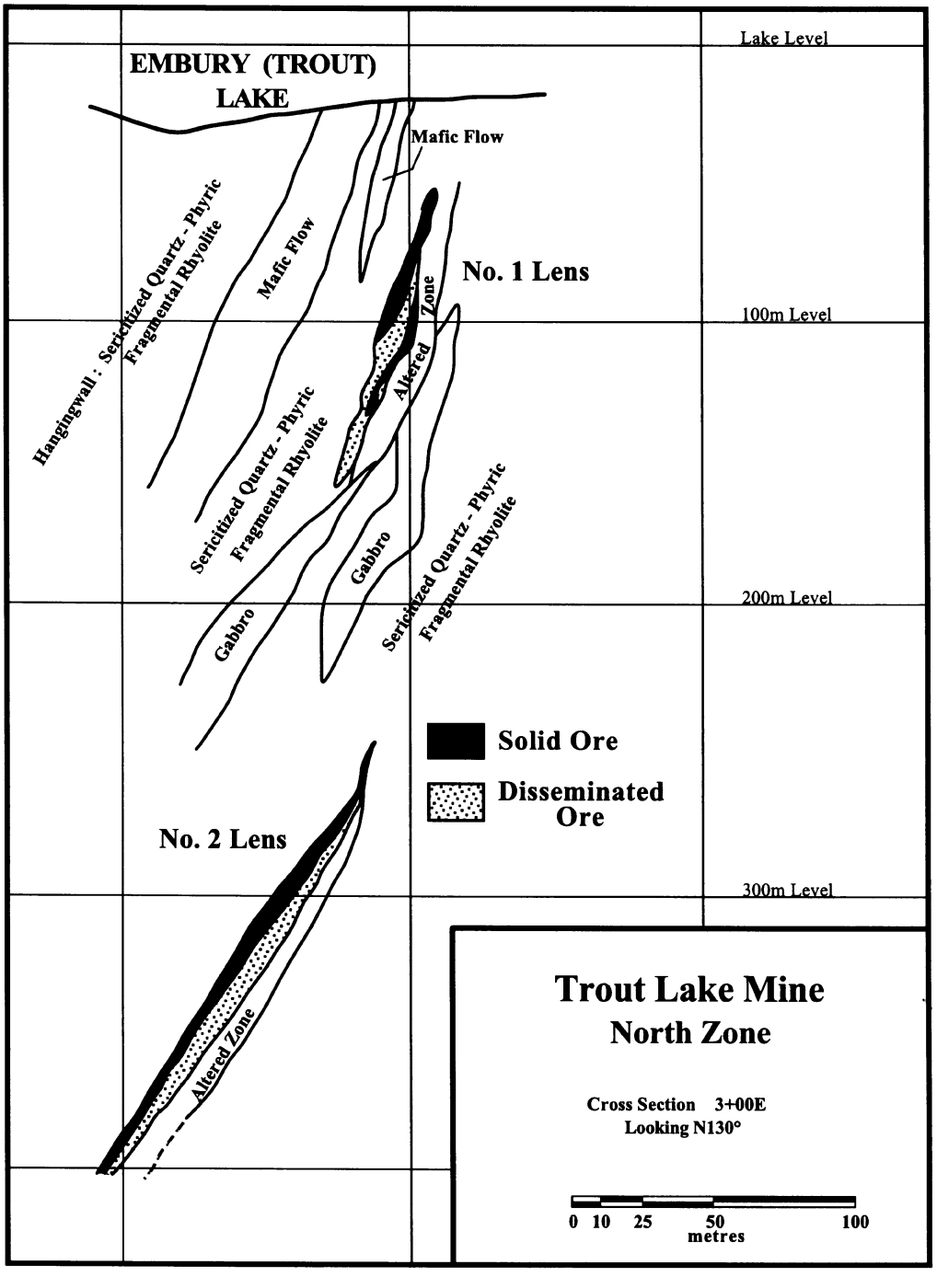

Fig. 2. Cross-section of the generalized geology of the Trout Lake mine (after Ko, 1986)

#4 lens sill pillar failure

The geology of the #4 lens consists of four main rock types: quartz porphyry (hangingwall), solid ore (ore zone), disseminated ore (ore zone), and chlorite schist (footwall). The quartz porphyry hangingwall comprises quartz with some muscovite and chlorite. The rock is fragmented, but cohesive, with the fragments being approximately 3 to 25 mm in width. The solid sulphide ore is predominantly pyrite with varying quantities of sphalerite. Solid sulphides make up approximately 50% (by volume) of the total ore, with disseminated sulphides making up the other 50%. The disseminated ore is mainly chalcopyrite and pyrite within a chlorite schist matrix. The footwall rock is a dark chlorite schist made up of alternating layers of quartz and chlorite, with veinlets of quartz-carbonate transecting the schist.

The mine production plan called for the #4 lens to be mined in two halves which were separated by a roll in the orebody where the dip steepened from 60 to 70°. During mining of the upper half of the lens (completed prior to 1992; Fig. 3), few ground control problems were experienced. However, during excavation of the lower half (January to October, 1992), hangingwall sloughs and some footwall slabbing were reported on almost every level. This was attributed to poor drilling and blasting, higher stresses and the foliated nature of the rock. More significant groundfall problems began to occur after completion of mining below the 420 m level (Fig. 3). Effectively, a pillar existed between the 420 m level and the 390 m level, with the exception of a development drift driven at the 405 m level. The division of this remaining ore by the development drift into two separate pillars (early 1993), resulted in an increase of stress concentrations in the pillar and possibly a reduction of the overall strength (which is a function of the pillar's width to height ratio). Ground control problems were observed on the 420 m level, most notably along the back (i.e. roof) of the undercut. Unravelling of the disseminated ore and slabbing of the chlorite schist footwall led to the stronger intact solid ore being left unconfined. This then led to gravity falls of large solid ore wedges (shaped by discontinuities in the solid ore), extreme mucking conditions and production delays. Cable bolting from the drift was performed, but the majority of these bolts snapped. The proposed failure mechanism is depicted in Fig. 4. As the disseminated ore progressively unravelled, large wedges continued to fall resulting in a decision to abandon the stope (late 1993).

Eventually, with the caving continuing to 'chimney' upwards, the failure will reach the excavations of the upper half of the stope. The cost of the failure was the loss of the remaining ore and the production time invested in the development of the stopes. However, the majority of the ore in the lens was recovered and the loss was not considered to be that significant. The possibility that with deeper mining and higher stresses this type of failure may reoccur, increasing mining costs and operational problems, warranted further study.

Laboratory testing

Laboratory testing provides a means to measure the response of rock to induced stresses. Determining this response is essential in mine design, since mining an orebody results in a constantly changing stress environment in the rock mass surrounding the opening. To

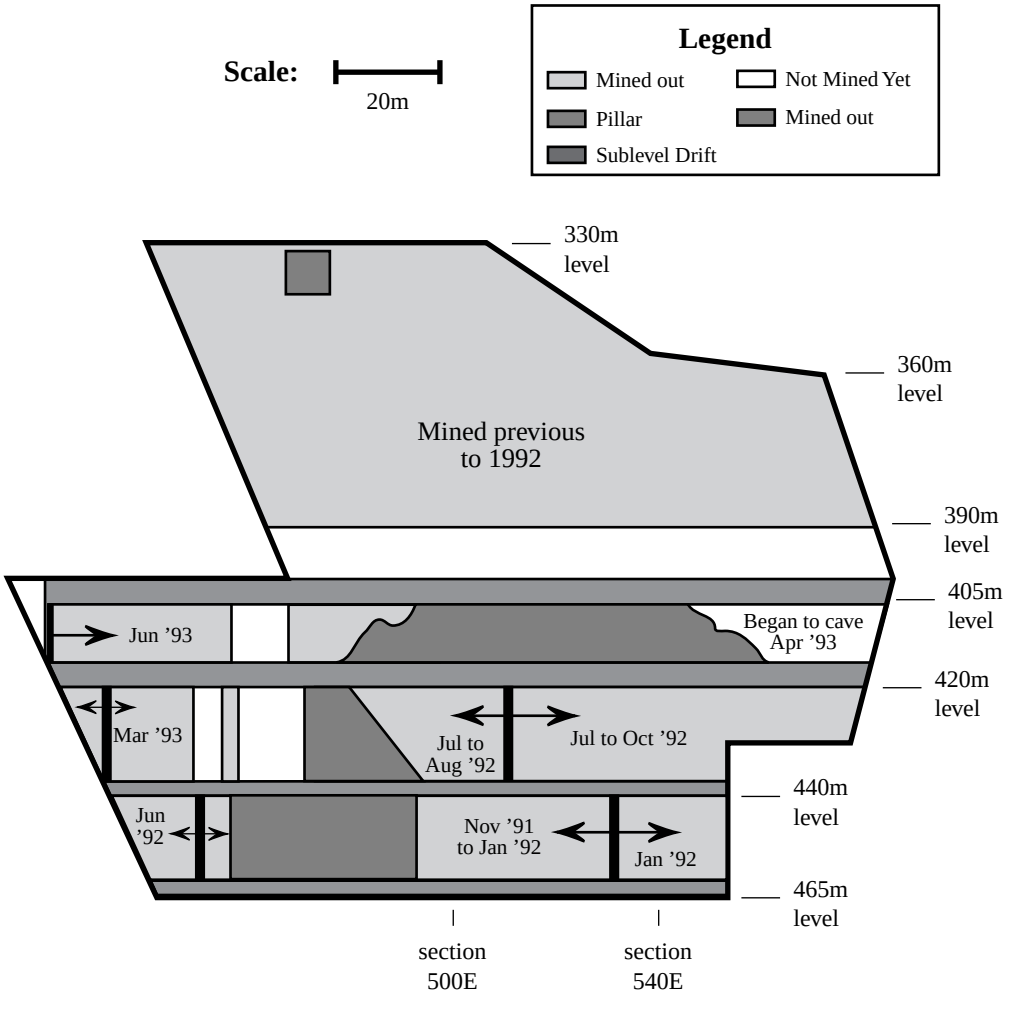

Fig. 3. Diagram showing the sequencing of the ore extraction for the #4 lens

study the effect that these induced stresses will have on the rock mass and whether it will be strong enough to support them, two elements are required: a constitutive relation, to describe how the rock will behave when subjected to a change in the stress field; and a failure criterion, to describe the strength of the rock.

Laboratory testing for the Trout Lake mine was carried out between May 1993 and August 1994 at the University of Saskatchewan Rock Mechanics Laboratory (Eberhardt *et al*., 1994). It was proposed that a series of laboratory tests be conducted to characterize the rock masses encountered at the Trout Lake mine and to determine the material parameters required for numerical modelling studies of underground mine-induced ground deformations. Laboratory testing involved the four main rock types found in the study area representing the footwall, the ore body and the hangingwall (chlorite schist, disseminated ore, solid ore and quartz porphyry).

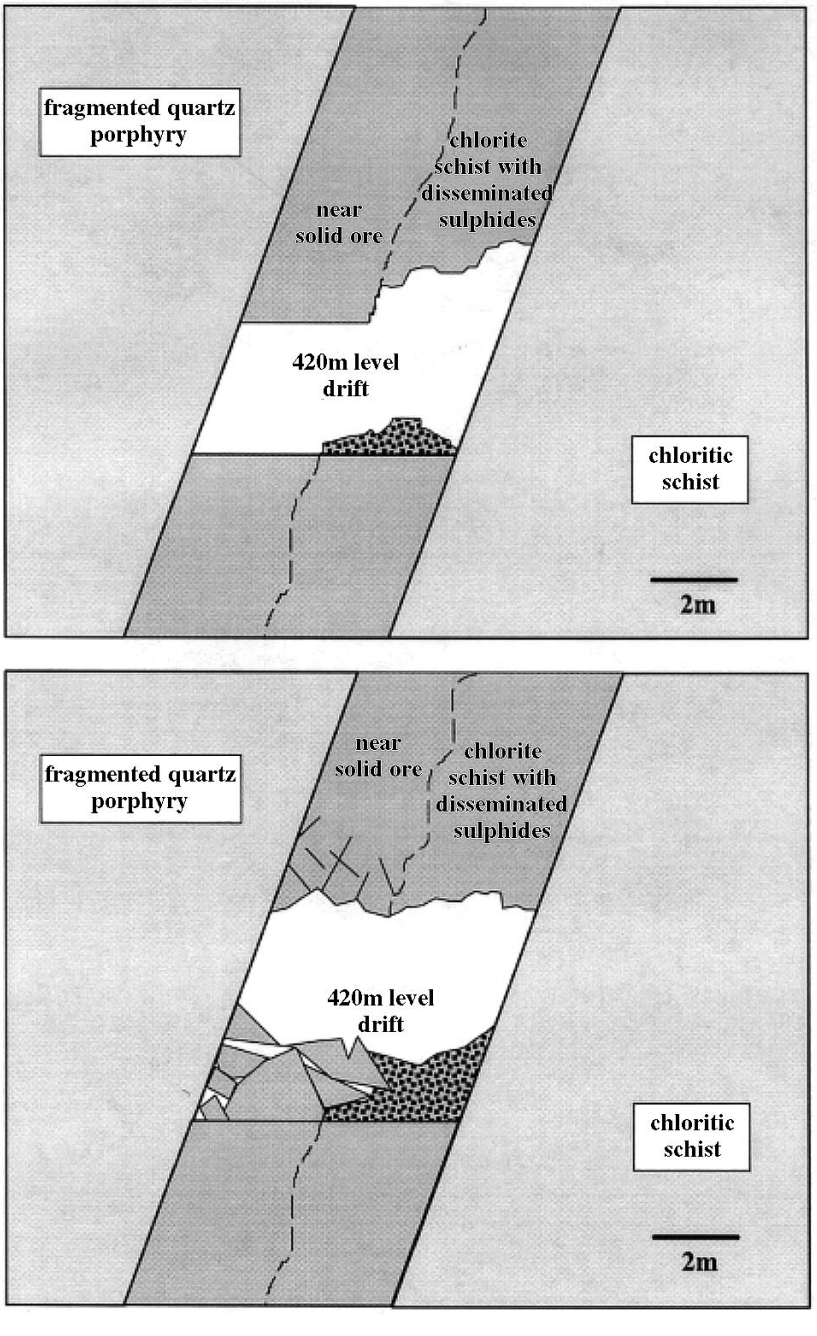

Fig. 4. Proposed failure mechanism in the #4 lens sill pillar. The upper diagram depicts the sloughing and 'working' of the disseminated ore. The lower figure shows the failure of larger solid ore wedges after the solid ore is left unconfined

Block samples were obtained from the mine from which 38.1 mm (1.5 in) diameter cores were drilled and marked for orientation with respect to foliation. In the case of the solid ore, samples were drilled at varying orientations since no noticeable foliation existed. Intact core samples retrieved from the blocks were then prepared for testing, according to ASTM standards.

Index tests

Index properties derived for the Trout Lake samples include porosity, density, slake durability, point load strength index and petrographic description (Table 1). From the index tests it can be seen that the solid ore samples have a much higher density than the footwall or hangingwall rocks. The density of the disseminated ore is between these values and varies depending on the amount of stringer ore present in the sample. The significantly higher density of the solid ore would, in most cases, indicate a much higher intact strength. However, observations made during the drilling of the samples suggests that the strength of the solid ore could be greatly reduced due to jointing. There is also fracturing in the disseminated ore and the quartz porphyry (which is known locally as a 'fragmented' quartz porphyry). This is confirmed by both visual observations and higher porosity values in the samples. There were difficulties in obtaining intact cores from blocks of solid ore, disseminated ore and quartz porphyry, due to these fractures. In the case of the chlorite schist two separate observations were made while preparing the samples. Firstly, the rock would sometimes break down when exposed to mechanical forms of erosion (water-cooled drills and saws). Secondly, unlike the other samples, cores did not break off along fractures but along foliation planes.

To determine the potential for breakdown, slake durability testing was conducted following ASTM standards. Results showed that slaking in the schist is minor with the test pieces remaining virtually unchanged. To determine the degree of foliation in the schist and its significance on the strength of the rock, point-load testing was performed in accordance with the ISRM's suggested methods (Anon., 1985). Testing was conducted on irregular lump specimens with the load being applied both parallel and perpendicular to the foliation. As would be expected, the schist split more easily along the foliation than across it. The point load anisotropy index, I_a (the maximum to minimum strength ratio), was calculated to be 3.4. Using the point-load strength anisotropy classification system proposed by Tsidzi (1990), the chlorite schist would be classified as a strongly foliated

Table 1. Laboratory rock index properties

Rock type	Density (g/cm^3)	Porosity (%)	Slake durability (%)	Point load index, Is (50) (MPa)
Chlorite schist	2.76 ± 0.01	0.3 ± 0.1	99.4 ± 0.1	1.8 ± 0.4 (parallel to foliation) 6.2 ± 1.8 (perpendicular to foliation)
Disseminated ore	3.03 ± 0.30	0.5 ± 0.2	n/a	n/a
Solid ore	3.99 ± 0.04	0.1 ± 0.1	n/a	3.8 ± 0.5
Quartz porphyry	2.67 ± 0.01	0.4 ± 0.1	n/a	n/a

rock. Comparatively, a weakly foliated rock such as a quartzite is given an I_a value of < 1.1. Using these results as a guideline, it was determined that the foliation should be given careful consideration during the design tests. Point-load testing performed on the solid ore provided lower than expected values, substantiating the observation that the rock is weaker than would normally be expected.

Design tests

Design tests were conducted to measure the quantitative material characteristics required for design calculations. These tests provided the deformation moduli required for constitutive models and the strength parameters required for failure criterion, and involve a number of different testing methods including uniaxial, triaxial, and Brazilian tests. In total, approximately 32 triaxial, 14 uniaxial, and 67 Brazilian tests were conducted (the number of Brazilian tests reflects the ease of preparation of the required disks). Of the three rock types tested which exhibited varying degrees of foliation (i.e. chlorite schist, disseminated ore and quartz porphyry), the chlorite schist displayed the strongest transverse elastic isotropy, with a Young's modulus 60% higher when loaded parallel to the plane of isotropy than when loaded perpendicular to it (Table 2). In other words, the chloritic schist behaves more stiffly when the principal stress direction is parallel to the foliation. Similar results showing a large difference in the deformability of a schist with respect to foliation have been shown by a number of authors, including Pinto (1970), Barla and Innaurato (1973), Kwasniewski (1983), and Read *et al*. (1987). This anisotropy due to foliation was also reflected in point-load testing. In quartz porphyry, in which the foliation is only slight, the difference between the two Young's moduli is only 5 GPa, less than the standard deviation. In such a case, it can be assumed, for practical purposes, that the quartz

Table 2. Laboratory derived static elastic constants

	Static elastic constants (units)				
Rock type	E_1 (GPa)	ν_1	ν_3	E_2 (GPa)	ν_2
Chlorite schist	82.4 ± 8.8	0.15 ± 0.02	0.30 ± 0.07	51.6 ± 7.9	0.30 ± 0.01
Disseminated ore	31.3 ± 5.6	0.10 ± 0.03	0.31 ± 0.08	40.6 ± 14.2	0.20 ± 0.06
Solid ore	74.8 ± 10.4	0.28 ± 0.05			
Quartz porphyry	53.4 ± 19.5	0.15 ± 0.10	0.34 ± 0.11	58.3 ± 6.0	0.22 ± 0.07
Quartz porphyry (assuming isotropy)	56.4 ± 8.5	0.25 ± 0.08			

E_1 = modulus of elasticity in all directions lying parallel to the plane of foliation.
ν_1 = Poisson's ratio of strain in the plane of foliation due to stress applied parallel to the plane of foliation.
ν_3 = Poisson's ratio of strain in the plane of foliation to strain in the direction normal to it, due to stress applied parallel to the plane of foliation.
E_2 = modulus of elasticity in the direction perpendicular to the plane of foliation.
ν_2 = Poisson's ratio of strain in the plane of foliation to strain in the direction normal to it, due to stress applied perpendicular to the plane of foliation.

Table 3. Laboratory derived intact rock strength parameters

Rock type (and orientation with respect to foliation)	Mohr–Coulomb criterion (linear regression)			Hoek–Brown criterion (Simplex)						Indirect tensile strength
	c (MPa)	ϕ (degrees)	corr.	m	s	σ_c (MPa)	σ_T (MPa)	σ_c/σ_T	resid.	σ_T (MPa)
Chlorite schist										
Loading direction perpendicular to foliation	23.7	39.0	0.89	8.3	1	100.8	− 11.9	8.5	604	17.2 ± 4.9
Loading direction parallel to foliation	24.4	43.0	0.66	12.5	1	108.1	− 8.6	12.6	4207	5.2 ± 1.4
All test data	24.6	41.3	0.67	10.7	1	106.5	− 9.9	10.8	5859	
Disseminated ore										
Loading direction perpendicular to foliation	25.0	19.8	0.90	2.3	1	71.1	− 26.7	2.7	184	n/a
Loading direction parallel to foliation	16.6	26.6	0.94	4.5	1	51.9	− 11.1	4.7	66	
All test data	22.1	21.6	0.80	2.7	1	64.9	− 21.5	3.0	724	
Solid ore										
All test data	18.0	59.4	0.65	38.7	1	133.2	− 3.4	39.2	31581	8.6 ± 2.2
Quartz porphyry										
Loading direction perpendicular to foliation	28.1	42.4	0.77	10.2	1	127.5	− 12.3	10.4	3934	n/a
Loading direction parallel to foliation	8.0	52.5	0.83	69.0	1	26.1	− 0.4	65.3	8716	
All test data	16.6	48.3	0.67	20.7	1	81.0	− 3.9	20.8	22654	

porphyry behaves more as an isotropic material than as a transversely isotropic material.

The testing methods often utilized to determine the various intact rock strength parameters include uniaxial, triaxial and Brazilian testing. In the case of the Trout Lake testing programme, uniaxial and triaxial testing were performed to determine the compressive strength and the Mohr–Coulomb and Hoek–Brown failure envelopes, and Brazilian testing was performed to determine the indirect tensile strength of the rock (Table 3).

Uniaxial compression testing showed that the disseminated ore was approximately 50% weaker than the other rock types. The solid ore proved to be the strongest of the four rock types tested triaxially. However, due to fractures and jointing in the solid ore blocks, the strength of the test specimens was greatly reduced when tested without any confining stress.

Rock mass classification and empirical design

Although laboratory testing provides strength values and deformation properties for the intact rock, the ultimate strength and deformation characteristics of a rock mass are governed by the characteristics of the naturally occurring fracture systems that occur in the rock mass. This can be seen from the standard deviation of the testing results, which show that a range of values may be possible for even small core samples from the same block. This is due to fracturing and other forms of anisotropy not accounted for in the laboratory testing. In some cases the intact values determined in the laboratory can be considered a fair approximation to *in situ* behaviour, but in most cases the quality of the rock mass as a whole must be taken into consideration.

To judge the quality and the behavioural characteristics of a rock mass as a whole, rock mass classification systems have been developed based on determining the primary rock mass parameters that affect the strength. The purpose of these systems is to assign a numerical or quantitative assessment of a particular rock mass that can be used as a design aid. Two of these systems that have received significant use in underground hardrock mines are the modified rock mass rating (MRMR) method (Laubscher and Taylor, 1976) and the Barton NGI or 'Q' system (Barton *et al*., 1974). To assess the stability of a particular stope design, empirical design methods have been developed which are based on the analysis and interpretation of a number of case histories, whereby common factors form the basis for the design parameters. Most prominent of these for open stope design and assessment is Mathews' stability graph method (Mathews *et al*., 1980).

Mathews' stability graph method

Mathews' stability graph method serves as one of the primary empirical design tools used at the Trout Lake mine to provide assessment of stope designs and support requirements. A number of authors have reported the successful implementation of the method in the design of stopes at a number of Canadian mines, including the Thompson mine (Niemi *et al*., 1987), Ruttan mine (Pakalnis *et al*., 1987), Chadbourne mine (Bawden and Milne, 1987), Golden Giant and Ansil mines (Bawden *et al*., 1989), Detour Lake Mine (Pakalnis *et al*., 1991), and the Namew Lake and Callinan mines (Reschke and Romanowski, 1993). Mathews' results, based on work by Reschke and Romanowski (1993) at a number of HBMS mines in the Flin Flon area (including the Trout Lake mine), show a good correlation between the data collected from stope backs (both stable and unstable) and the stability design guidelines (Fig. 5a). Contrasting these results are the ones obtained in the analysis of HBMS hangingwalls (Fig. 5b) in which the field performance of hangingwall surfaces does not correlate well with the type of behaviour predicted by the stability graphs.

The poor correlation in the hangingwall analysis may help to distinguish which factors influence the degradation of the rock mass quality, and in addition are not being properly accounted for in Mathews' analysis. In the case of the hangingwall analysis, a larger exposed or unconfined area is involved as opposed to the smaller area analysed in the case of the stope back. With a larger area, the hangingwall becomes more susceptible to such factors as drilling and blasting, factors which may not be properly accounted for. Drilling can have a critical destabilizing effect when it results in the undercutting of the hangingwall structure (this is later demonstrated using the boundary-element numerical

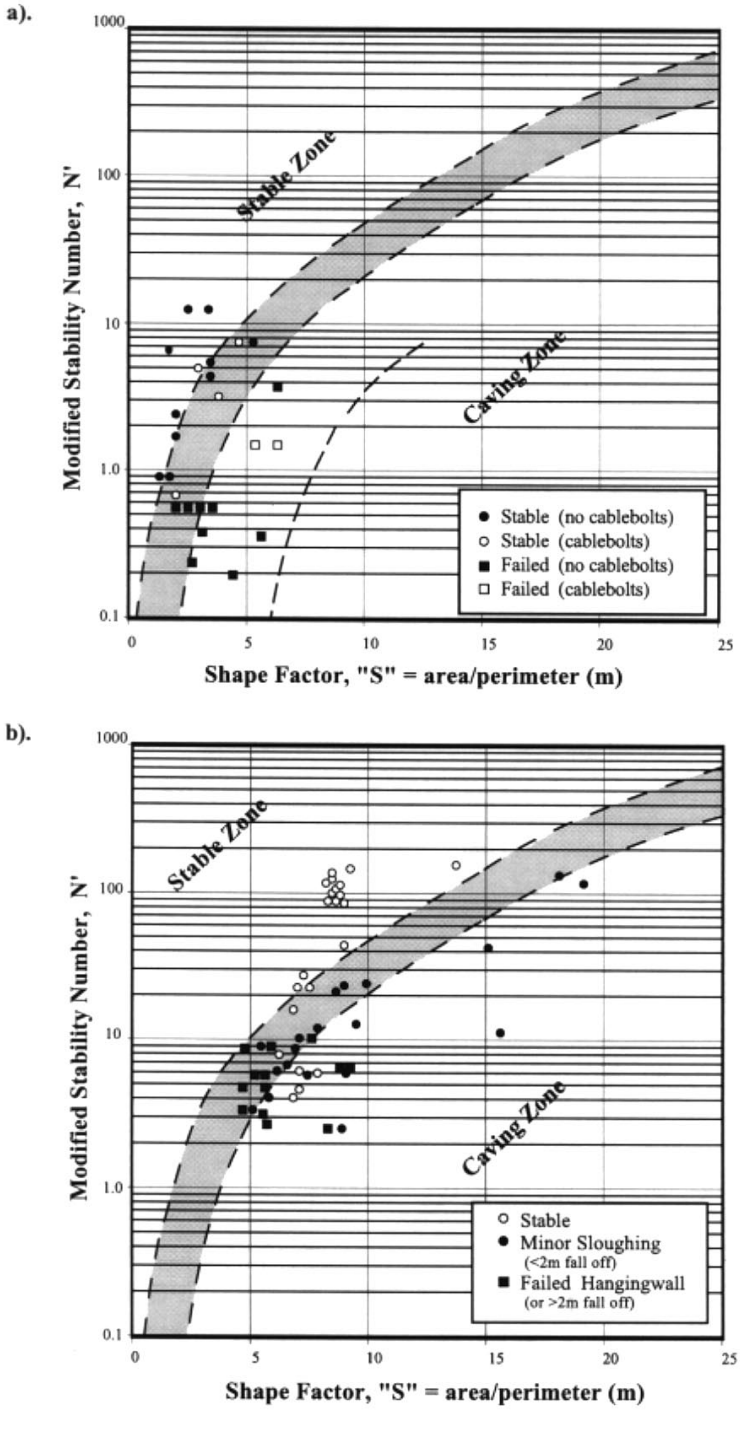

Fig. 5. Stability performance of (a) stope backs and (b) hangingwall at HBMS (after Reschke and Romanowski, 1993)

modelling method). Undercutting is not just the result of drillhole deviation but can also occur due to irregular geometries in the orebody. Reschke and Romanowski (1993) note that the Trout Lake sulphide deposits are highly sheared and the orebodies themselves exhibit a high degree of undulation, thereby requiring closely spaced diamond drilling to accurately define the hangingwall.

If there is an unexpected change in the hangingwall contact as compared with the geological model or deviation of drill holes into the hangingwall rock mass, the result is damage to the hangingwall and increased slough of waste into the stope. Blasting may also have an adverse effect on the quality of the rock mass, causing damage through strain-induced fracturing and/or gas penetration mechanisms. Strain-induced fractures, formed by tensile fracturing of the rock, result in the creation of new fractures and the extension of old ones, possibly forming wedges with other fractures or existing structural discontinuities. To reduce this problem of blast-induced damage at the Trout Lake mine, considerable effort has been directed at optimizing blast patterns and explosive type.

Scaling laboratory test values to in situ values

Laboratory testing deals with the determination of the physical properties of a certain rock type using samples varying from approximately 40 mm to 150 mm in diameter by 80 mm to 300 mm in length. By increasing the specimen size, certain anisotropic features may be incorporated such as a single fracture or discontinuity in a larger core sample, multiple discontinuities in a block sample, or faults and multiple joint sets in a rock mass. Determination of the physical properties of a rock mass through large scale or *in situ* testing may therefore seem more reasonable. However, larger samples are more difficult to gain access to, more costly and difficult to prepare, and the result of preparing the sample for large-scale testing may result in an exaggerated observation of the actual scale effect which might have only been minor (Barton, 1990).

In either case, whether the testing is small or large scale (*in situ*), the question of sample disturbance and damage must also be addressed. The variability of some of these results demonstrate that there are a number of factors which may influence the results of both laboratory and *in situ* testing. Since testing, in both cases, involves material found at depth, effects such as microcracking and fracturing due to blasting and induced stresses must be considered for their effect on altering the physical properties of the rock. The degree of these effects will be dependent on such factors as the blast-hole density and charge weight per delay, *in situ* stresses and rock strength. For example, Martin (1993) has shown that intact samples obtained from a pre-stressed medium suffer irreversible damage when the far-field stresses exceed as little as 15% of the rock's compressive strength. Considering the number of factors which may influence the results of both laboratory and *in situ* testing, it is necessary to accept laboratory and empirical values as a component in the overall design plan, altering them accordingly to take into account scale effects and sample damage.

Within the scope of this study, scaling of the laboratory properties obtained for the four Trout Lake rock types will be controlled by two factors: the attributes of the rock mass and the design method being utilized. The design method being used in this study is numerical modelling, and because different numerical methods allow for different assumptions to be made concerning the behaviour of the rock mass, adjustments to the material properties

will differ from method to method. However, certain generalizations can be made concerning the attributes of each of the four rock masses under study using both the laboratory testing and the rock mass classification work:

1. Even though samples for each rock type were taken from the same block, the results obtained through laboratory testing showed a range in values. This provides an upper and a lower range of values representing different levels of competency (or damage) in the blocks and the rock mass. The laboratory values can therefore be looked at as an approximation of how the rock mass will behave, so that in the design stage, a range of answers may be necessary to predict how the rock mass will respond to a change in the stress field.
2. Structural mapping has shown that two major and two minor joint sets exist in the orebody. These discontinuities could also be seen in the solid ore block and in some of the individual samples. Observations made during the testing of the solid ore showed that, in some cases, movement along fractures occurred throughout loading up to the point of failure, which occurred at stresses much lower than samples that displayed no sign of natural fractures. Because a strength range of over 100 MPa exists between some of these tests, it can be assumed that the lower range is a good approximation of a jointed rock and the upper range is a good approximation of the intact rock.
3. Even though the quartz porphyry hangingwall is heavily fragmented, the rock is still cohesive as a whole. As can be seen by Mathews' stability plot (Fig. 5b), the majority of the hangingwalls are stable. Mine personnel consider the hangingwall rock as being 'fairly competent', blaming any failures or sloughing on poor drilling or blasting practices.
4. Poor blasting techniques have been partially responsible for some stability problems in the mine. To account for this, the strength properties of the rock immediately surrounding the excavation may be reduced. It would be assumed that farther away from the opening, there is less damage to the rock due to blasting and the corresponding strength properties are higher.
5. Failures in the chlorite schist footwall are mainly controlled by the foliation, a property of the rock represented reasonably well in the laboratory tested samples.
6. Using these assumptions, the properties derived from the laboratory testing can be judged as to their accuracy and whether any scaling is required to represent the rock mass as a whole more accurately. In addition, parametric studies performed through numerical modelling allow for the investigation of the effect of scaling laboratory test values.

With a more comprehensive *in situ* characterization, a better understanding of the rock mass would be possible. However, with limited resources, mines usually have to use the most cost-effective data attainable. The laboratory testing performed provides a reasonable approximation of the physical properties of the different rock masses. The rock mass characterization then allows for other forms of anisotropy (which may be missed by the laboratory testing due to scale) to be accounted for. Adjustments to the laboratory test data, to be used in the numerical models or other design methodologies, can then be made on a case-by-case basis.

Numerical modelling

Many design problems in rock mechanics involve a complex interaction between such parameters as irregular geometries, anisotropic media and non-linear constitutive behaviour. In such cases, conventional methods of analysis, which are usually based on analytical solutions, are impractical due to the large number of simplifications that are required to make the problem determinate. Numerical modelling design methods do not require such gross simplifications and therefore provide a means to solve these more complex problems. In addition, a number of different numerical methods and modelling packages are available, giving the user more control over the simplifications and assumptions that are made in the analysis of a given problem. This allows for control and balance between the amount of detail required to represent the problem properly and the amount of time available to solve it effectively.

The general procedure used by most numerical methods to solve a given problem is to divide the problem into smaller physical and mathematical components and then sum the influence of the components to approximate the behaviour of the whole system (Hoek *et al*., 1991). The manner in which these equations are formed and solved differentiates the techniques. These methods can be subdivided into two main categories: integral (boundary) methods and differential (domain) methods. Integral methods involve the discretization of a surface and the application of equations to it, thereby reducing the dimensional order of a problem. Differential methods involve the division of the problem domain into a set of elements, to which a set of governing equations can be applied. Hybrid methods which link parts of the differential and integral methods have been developed to exploit the advantages of both methods. This linking of solution schemes allows for the far-field rock to be modelled as an infinite domain using boundary elements, and the more complex constitutive behaviour of the near-field rock to be modelled using the differential method. Another method which is commonly used in situations where discontinuities play a major factor in the design problem is the distinct-element method, developed by Cundall (1971), which is designed to treat a discontinuous rock mass as an assembly of quasi-rigid blocks interacting through deformable joints of definable stiffness. This method does, however, require a sufficient knowledge of the nature of the discontinuities within the modelled region.

The integral and differential methods incorporate different assumptions and simplifications into their respective solution processes, thereby resulting in advantages and disadvantages when compared to each other. In addition, the integral and differential methods can be regarded as being two general types of numerical methods which can be further broken down into four primary methods. These include the finite-difference and finite-element methods (differential methods), and the boundary-element and displacement-discontinuity methods (integral methods).

Each of these four methods has been widely used to analyse stress conditions around openings and make assessments of stope designs and specific ground failures, with the general approach being the selection of a single method which is best suited for the particular environment. In some cases, the respective authors acknowledge the existence of the other methods but rely on one specific method, citing certain advantages in it (Brady, 1977; Brummer, 1985; Spottiswoode, 1990). In other cases, authors have used two different methods to analyse a problem, but only as a comparison, the end result being to recommend one method over the other (Hart, 1980; Brady and Johnson, 1989). Usually the

method is chosen based on the programme's capabilities and complexities, the cost, and availability of the programme, and/or the time required to gain a working knowledge of it.

With increasing experience and the development of different numerical methods over the past 20 years, the approach of selecting just one method best suited for the problem should no longer be required. Instead, an approach where several different methods are used in conjunction, allowing for the advantages of each method to be utilized, would seem to provide the ideal design strategy. To show how such an approach allows for a comprehensive analysis of the different perspectives of stope design and analysis, modelling of the Trout Lake case study of the #4 lens sill pillar failure was completed.

The boundary-element method

The boundary-element method involves the discretization of a surface for which a set of equations are written relating displacement components to traction components. The remainder of the domain is treated as being infinite or semi-infinite. This greatly reduces the amount of input data required and makes this method an extremely efficient tool for the analysis of stopes. A large number of authors have used boundary-element methods to design stopes (Brady, 1977; Bawden and Milne, 1987; Beer, 1988; Grant *et al*., 1993). A major limitation of the method is that linear material behaviour and homogeneous material properties are assumed. Although a non-linear, inhomogeneous, anisotropic material behaviour is more realistic, its use would negate the intrinsic advantages and simplicity of the boundary-element solution.

Simple two-dimensional elastic analysis

In view of the limitations in effectively representing the reaction of a complex material, the use of the boundary-element method in the design plan should capitalize on its speed and efficiency. These factors are best utilized in providing estimates of stress concentrations induced in the rock mass by an excavation due to its geometry. Cross-sections through the stope were constructed to show how the relative stress concentrations would be effected by the different excavation geometries. Results of a 2-D boundary-element analysis using the program EXAMINE^{2D} (Curran and Corkum, 1988) showed that the highest stress concentrations occur along a 40 m stretch of the sill pillar on the footwall side.

This agrees with the location of the actual failure indicating that the geometry of the stope may have been an important factor in the resulting failure. Further analysis shows that adjusting the shape of the stope by reducing the span of the back (i.e. reducing the sharpness of the angle between the roof and the footwall) results in a significant decrease in the stress concentrations (Fig. 6). Such revisions to the final stope geometry are possible throughout the mining cycle of the stope because of the quickness and ease with which models can be created and solved by the boundary-element method. These results also show how important is accurate drilling, since even minor deviations can result in problem geometries that are prone to large stress concentrations and hence are more susceptible to failure.

It should be noted that the sensitivity of these models to the material input parameters (i.e. Young's modulus and Poisson's ratio) is insignificant in terms of stress concentrations

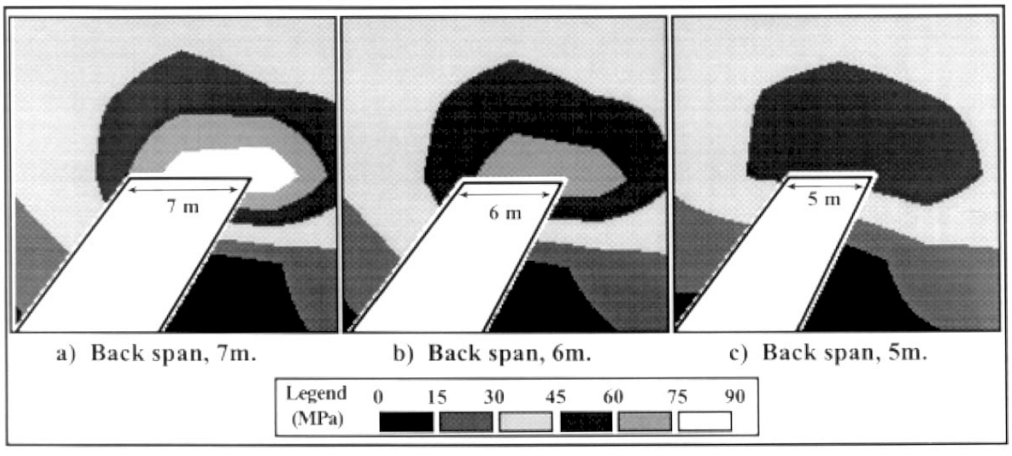

Fig. 6. Effect of reducing the span of the back on the major principal stress (σ_1) concentrations

since the stress field calculations are dependent only on the initial stress field (which for this case was estimated as $\sigma_V = 11$ MPa, $\sigma_H = 22$ MPa at 420 m depth), the unit weight of the host rock, and the geometry of the excavation. The elastic moduli are, however, part of the displacement calculations. The material input values typify the values obtained for the quartz porphyry which makes up the majority of the host rock.

Three-dimensional analysis

The user-friendliness of programs like EXAMINE^{2D}, combined with the computational efficiency of the boundary-element method, has aided in the development of 3-D codes which are gaining widespread use. Two-dimensional models require the assumption of plane strain and are therefore inadequate if 3-D effects are considered to be significant or crucial to the design plan. In the case of an open stope, the 3-D analysis allows for a more accurate representation of the near-field stress concentrations that develop around the ends and edges of the stope. However, like its 2-D counterpart, the 3-D boundary-element analysis requires the assumption of a linear elastic material, thereby providing an inadequate representation of an anisotropic or discontinuous rock mass.

A 3-D analysis of the study area was performed using the program EXAMINE^{3D} (Curran and Corkum, 1993). The objective of the first part of the study was to analyse the effects that the surrounding excavations may have on the #4 lens. Brady and Brown (1993) determined that the 'zone of influence' of a circular opening was five times its radius, beyond which the pre-mining or virgin stress field would not be significantly affected. In the case of a stoping operation, in which numerous large openings are present, the determination of the zone of influence is more complicated. The efficiency of the boundary-element program allows for such checks through the construction of large models which can incorporate the entire mine. Such a model was constructed to include all of the mined-out stopes of the Trout Lake 'north' zone between the 300 m and 500 m level. The results of the model showed that although the excavation of the individual stopes influences the stress fields in the near-field, their extraction does not have a

significant influence on the study area in question. These results justify the assumption in later models that the surrounding excavations do not have a significant effect on the #4 lens. This allows for other models to be simplified since the inclusion of surrounding excavations is not essential. A further advantage to this type of analysis is that a check can be performed well ahead of excavation, based on exploration data, to determine if any highly stressed zones are to be expected from the interaction of neighbouring excavations.

The second phase of the 3-D boundary-element analysis involved the modelling of the #4 stope so as to check the effectiveness of a 2-D analysis. Using the same input parameters as used in the 2-D analysis, the examination of the 3-D geometry allows for a check on the validity of the 2-D assumption of plane strain. The assumption of plane strain requires that strains be restricted to a single plane. Therefore, this assumption is most applicable when the conditions of a problem are such that they involve the geometry of a body loaded uniformly over a comparatively long distance in one direction. Although this assumption can be regarded as being adequate in the modelling of a tabular orebody (Crouch and Starfield, 1983), the irregular geometry that is present in the third dimension requires some consideration. A comparative analysis of the 2-D and 3-D modelling (Fig. 7) shows similar results with respect to predicting a higher stress concentration in the vicinity of the actual failure (i.e. in the pillar directly above the lower half of the mined out stope). To allow for direct comparisons between the 2-D and 3-D results, the stress grid spacing, which dictates the resolution of the stress calculations in the problem domain, was adjusted so that it would be identical for both models. A direct comparison of the 2-D sections is provided in Fig. 8 using sections through the 3-D model which mirror the cross-sections modelled in 2-D. This comparison shows that although both models predict a similar pattern in the stress field, the magnitude of the stresses calculated in the 2-D model are approximately 40% higher than those found by the 3-D model. Similar comparisons have been made by Pariseau and Duan (1987), who found that their 2-D finite-element models exhibited stresses 33% higher than their 3-D finite-element models. Conceivably, higher stresses should be expected in 2-D models since 3-D models allow for the redistribution of stresses in the third dimension. In other words, the 3-D models allow for the stress concentrations to be partially dissipated in the third direction, whereas the 2-D models restrict the stress redistribution to act only in the plane of analysis. This shows that 2-D modelling can overestimate the resulting stress field around an opening, thereby making it a more conservative estimate of induced stresses.

Displacement-discontinuity method

The displacement-discontinuity method, a particular kind of boundary-element method, is based on the analytical solution to the problem of a constant slot-like opening, or discontinuity, in displacement over a finite line segment of an infinite elastic solid (Crouch and Starfield, 1983). The solution is found by solving for the displacements along an element to coincide with the distribution of tractions applied to the discontinuities' surfaces. This solution is similar to the boundary-element method, with the exception that a displacement-discontinuity element represents a pair of opposing surfaces separated by stiffnesses (or springs), instead of one surface as in the case of the boundary element method. As a result, the method provides a pseudo 3-D analysis and is ideal for the

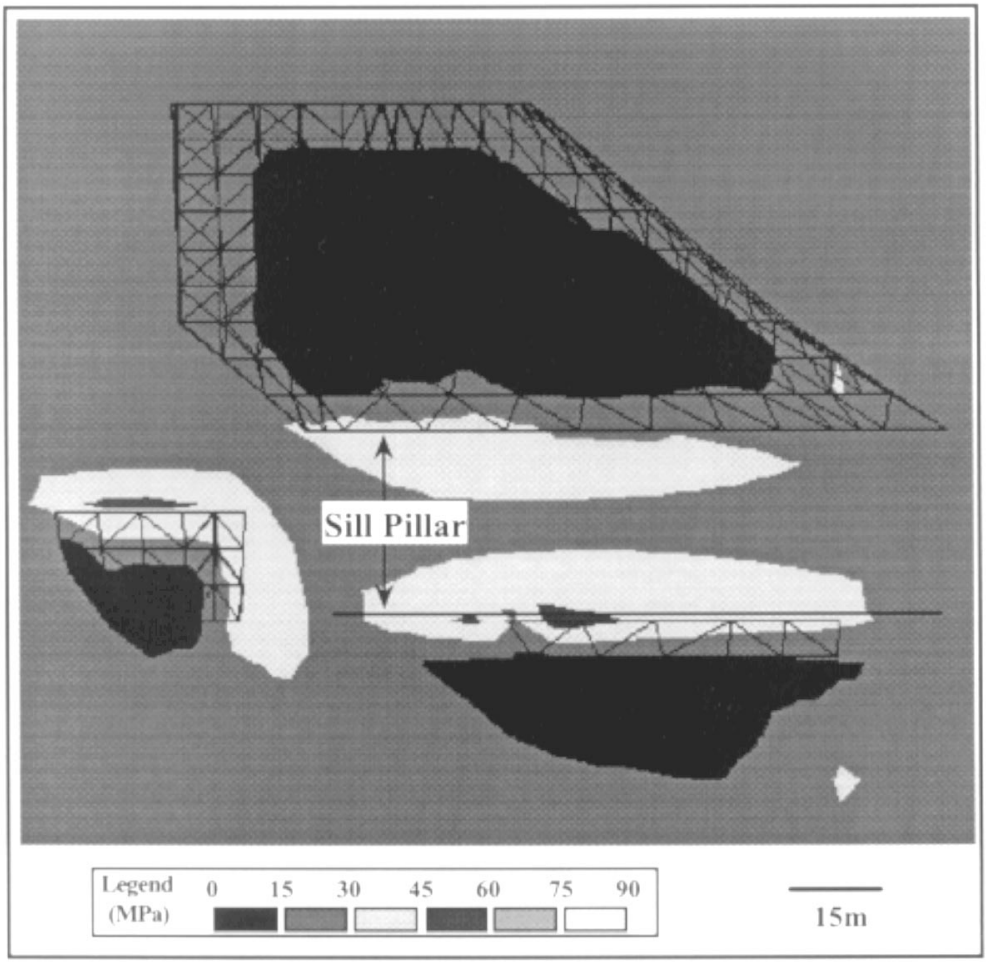

Fig. 7. Longitudinal section through the centre of the #4 lens, showing the major principal stress (σ_1) concentrations in the sill pillar resulting from the current state of excavation

analysis of excavations where the excavation surfaces are close together in relation to the surrounding medium, as in the case of a coal seam or a tabular orebody (Pande *et al.*, 1990).

Pseudo 3-D elastic analysis

The first apparent advantage of the displacement-discontinuity method is its ability to work in three dimensions requiring minimal effort for data input by the user. The displacement-discontinuity formulation also allows the boundary-element method's required assumption of material isotropy to be taken one step further. Although the method still requires the domain (i.e. host rock) to be modelled as an infinite elastic material, the unique

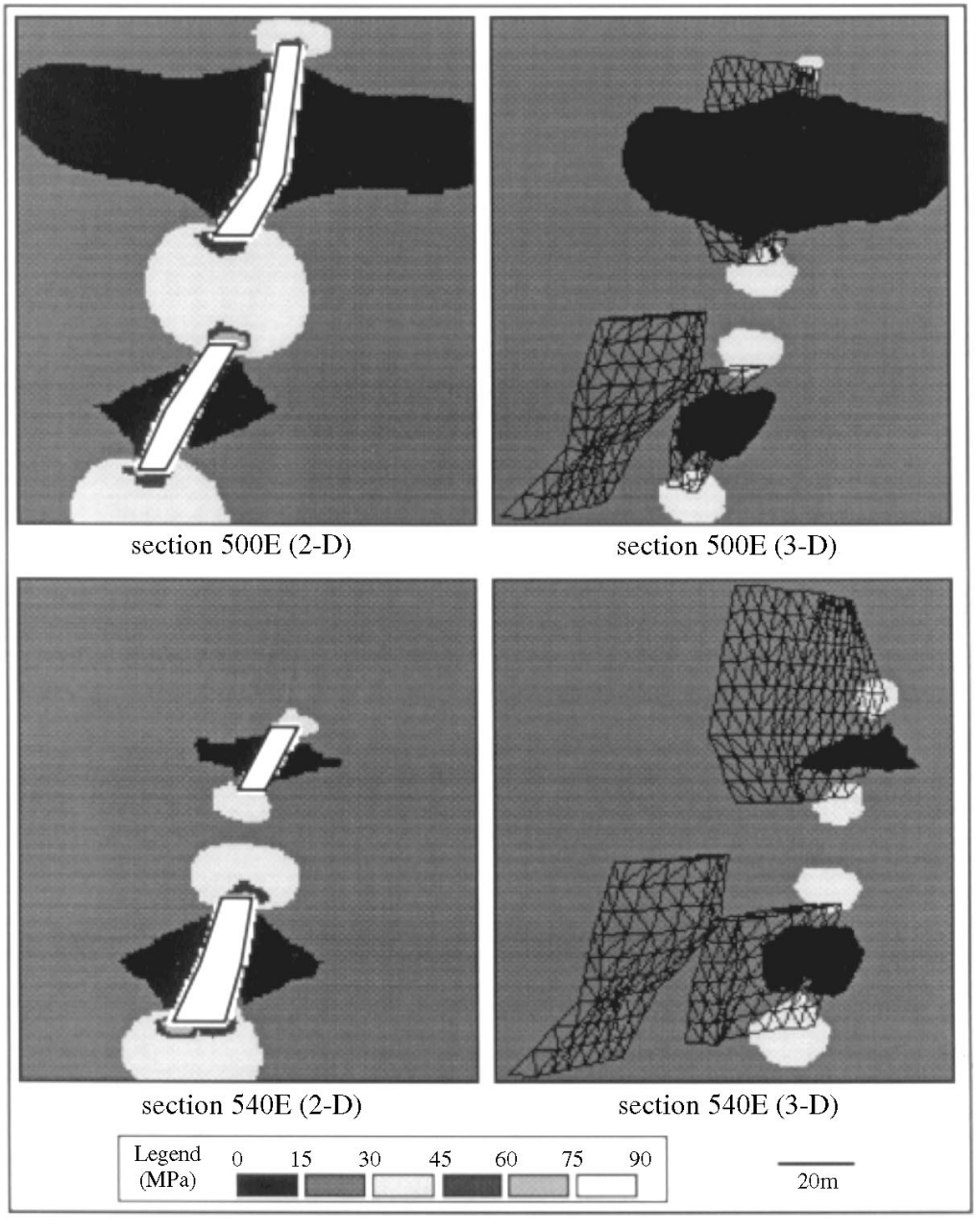

Fig. 8. Direct comparison of 2-D and 3-D boundary-element modelling showing major principal stress (σ_1) concentrations through the 500E and 540E cross-sections

formulation allows for the orebody (i.e. pillar material) to be modelled as a non-linear material. Results using the displacement-discontinuity packages MULSIM/NL (Zipf, 1992a, 1992b) and EXAMINE^{TAB} (Curran *et al.*, 1990) are comparable, showing increased stress levels in the pillar above the area of failure, with normal stress magnitudes equal to approximately 60 MPa. However, as elastic models, these results do little more than confirm the results found in the 3-D boundary-element analysis. Since EXAMINE^{3D} is a true 3-D program, the 3-D boundary-element results can be regarded as a more realistic portrayal of the elastic 3-D problem.

Pseudo 3-D elasto-plastic analysis

Despite the similarity of the displacement-discontinuity method to the boundary-element analysis as a tool for modelling linear elastic problems, its unique formulation does allow for some interesting and useful analysis. Through the method's portrayal of the problem domain as a slit in an infinite linear elastic rock mass, the use of stiffnesses between the two surfaces of the slit, representing the in-seam material, allows for various non-linear material models to be used. This provides both a pseudo 3-D and a pseudo non-linear material analysis. Using the program MULSIM/NL, models were created to represent the orebody material as both a linear elastic and a non-linear elasto-plastic material. The input for the elasto-plastic model requires a yield point to be determined and entered as a peak stress and a peak strain. The yield points and plastic moduli for the ore material and the near field rock material were taken as the average of the values obtained through laboratory testing.

Detailed modelling of the sill pillar (Fig. 9.) using MULSIM/NL allows for an additional fine mesh to be added in areas of importance. When run elastically, the model provided typical results for an elastic material, with the induced stresses being at their highest levels at the excavation boundary and decreasing in magnitude away from it (Fig. 10a). The elasto-plastic model provided more interesting results, showing that the stress concentrations in the pillar and relative magnitude can be significantly altered by any yielding in the rock mass (Fig. 10b). Next to the opening, where stress conditions are considered to be uniaxial (i.e. the other two components of the stress field have been effectively reduced to zero), a destressed zone appears, representing rock which has yielded due to the normal stresses exceeding the deviatoric yield point ($\sigma_1 - \sigma_3$). From the model, this is shown to be approximately 60 MPa. This correlates well with observed plastic failure around an opening, as opposed to elastic deformation in which the stresses would continue to increase, regardless of rock mass strength. Immediately adjacent to this yielded zone is a small region where the normal stress has reached magnitudes of 80 MPa. Although the induced stress in this area is significantly greater than the 60 MPa yield limit where rock mass failure is predicted, the increases in the σ_2 and σ_3 stresses have resulted in a deviatoric stress that is lower than the yield point and, therefore, an intact or non-yielded rock mass. The end result is that the higher stress contour effectively outlines the new pillar boundary (i.e. stable rock mass that has not reached its full load-bearing potential). The resulting 'hour-glass' shape of the pillar typifies observations made regarding pillar failures in coal and potash mines. In a detailed study of the failure process in coal pillars, Wagner (1980), showed that the failure commenced at the pillar boundary and migrated towards the centre where the core of the pillar had not reached its full load-bearing potential. Stresses throughout the pillar replicated this pattern with a destressed

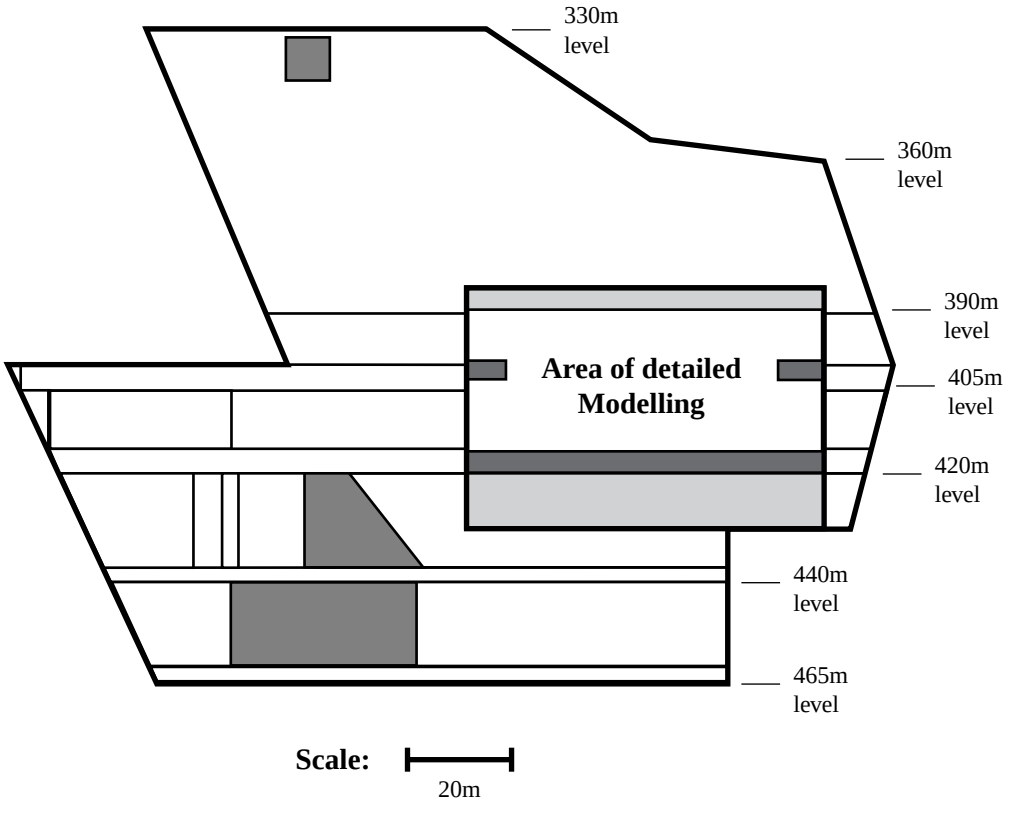

Fig. 9. Area covered by fine mesh in MULSIM/NL detailed modelling

zone in the yielded areas, a high-stress zone at the boundary between the yielded and the stable material, and a gradual reduction in stresses towards the centre of the pillar (Fig.11). Although the long axis of most coal-mine pillars is vertical as opposed to horizontal, as is the case in stoping operations, it can be noted that in both cases the maximum principal stress is parallel to the long axis. These findings, although significantly controlled by the input parameters describing the yield point of the rock, and in turn the extent of the yield zone, show that in the case of the #4 lens, the splitting of the sill pillar in half by the development drift, significantly increases the volume of yielded material, effectively reducing the volume of stable or intact material (i.e. the pillar).

Analysis of mine excavation sequencing

Another useful feature of the displacement-discontinuity method is the ease with which it allows the analysis of progressive mine sequencing and the subsequent evaluation of intermediate results. This feature enables the user to examine stress and displacement changes as the mine develops. Such changes more readily compare with field measurement data that tend to measure changes in stress and displacement (convergence) as opposed to total or absolute stresses and strains. In addition, the multiple mining step feature decreases

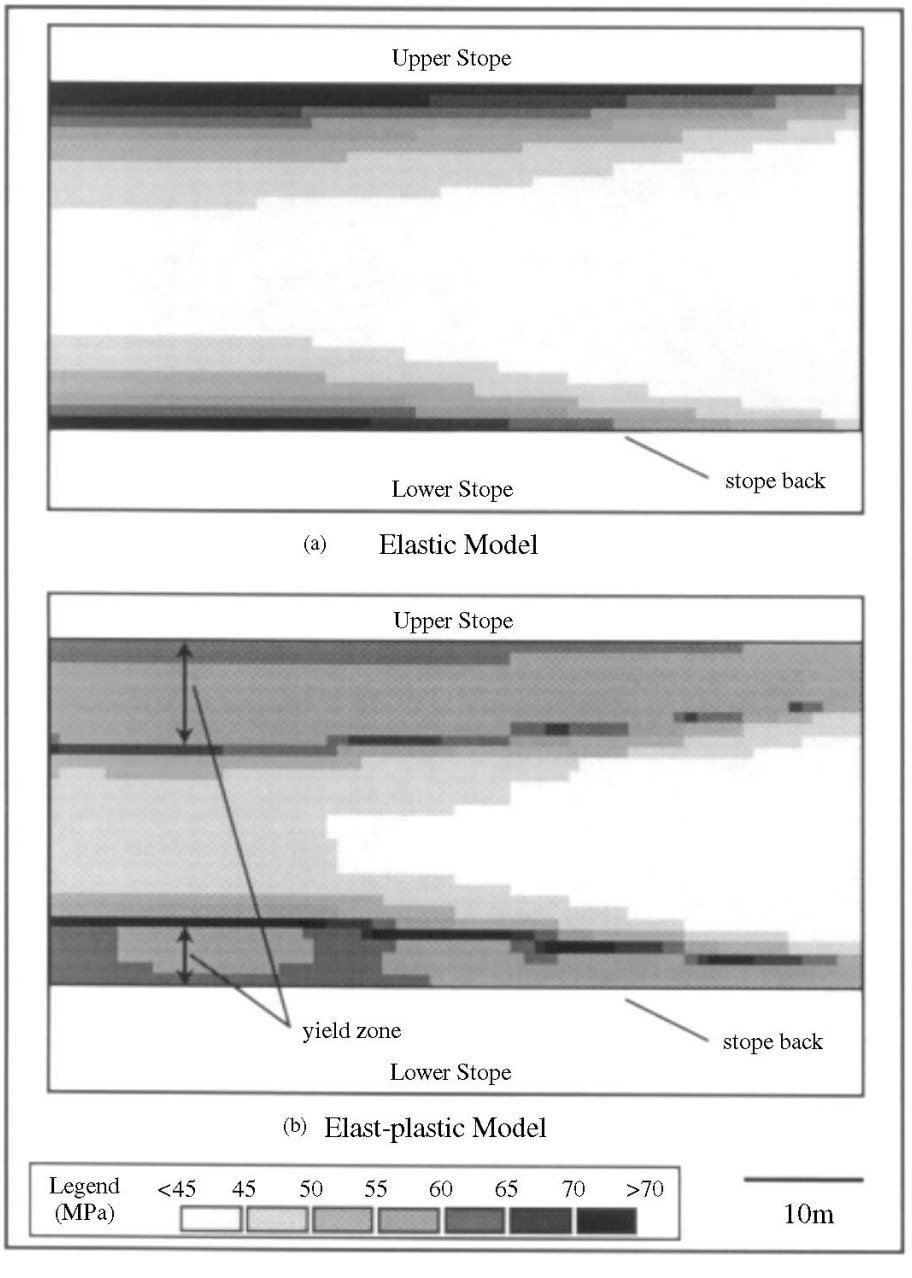

Fig. 10. MULSIM/NL linear (a) elastic and (b) elasto-plastic results. Plots show normal stress contours along a longitudinal projection of the pillar area

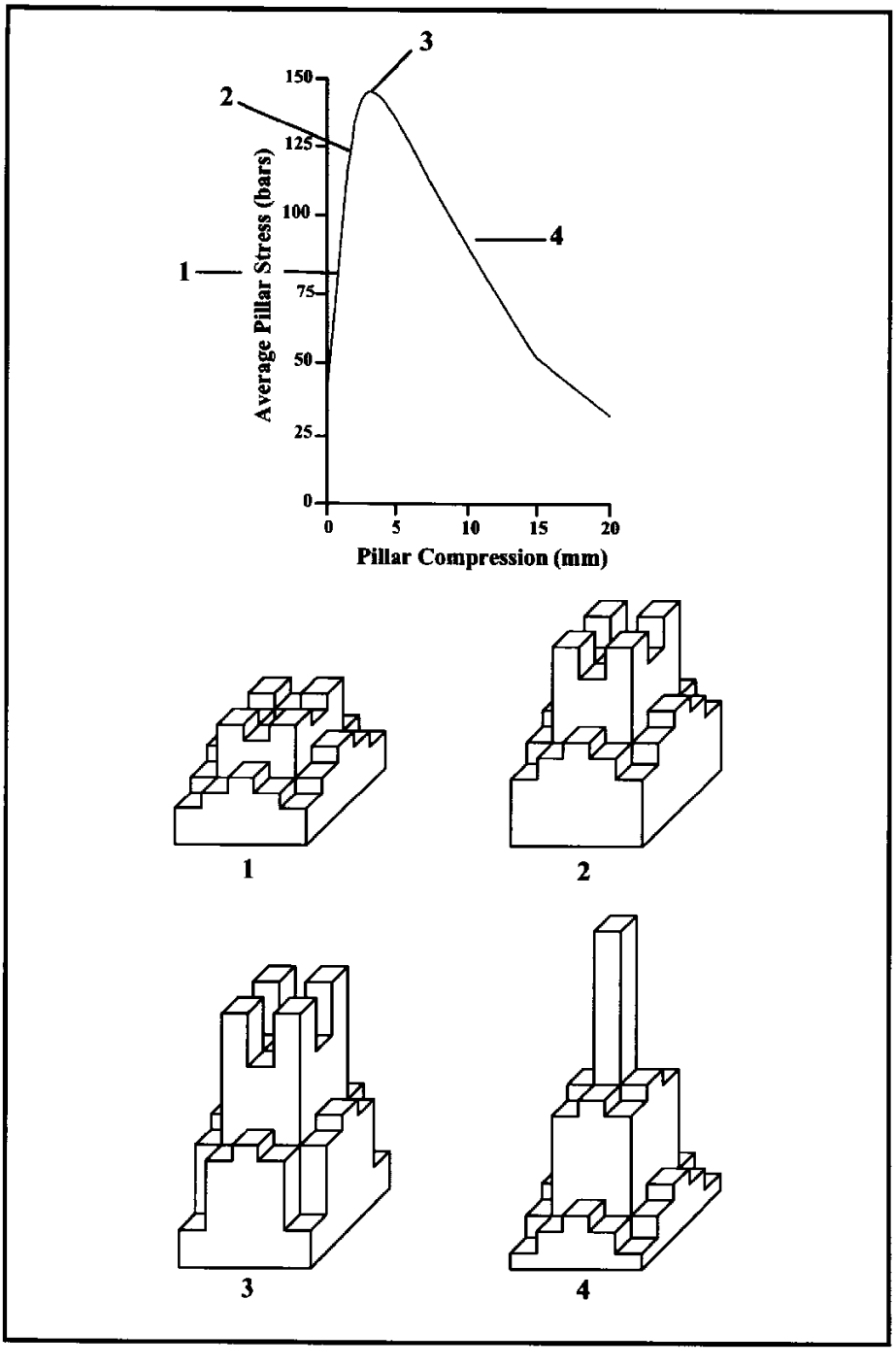

Fig. 11. Distribution of vertical stress in a coal pillar at various stages of pillar failure (after Wagner, 1980). Column heights denote the relative stress magnitudes found in different regions of the pillar

computing time since the computed stresses and displacements for one step become the starting point for the solution of the next step in the iterative equation solving process.

Each of the MULSIM/NL and EXAMINE^{TAB} models were created duplicating the actual excavation sequencing used in the mining of the #4 lens. Limited to linear elastic analysis, EXAMINE^{TAB} makes this process extremely easy, allowing for a number of excavation strategies to be modelled in a relatively short time. In addition to the actual sequencing pattern used, two alternative sequencing patterns were analysed. The first alternative sequencing plan closely followed the actual mining plan, except in the vicinity of the failure area where the direction of mining was simulated to occur from east to west (or inwards towards the failed area) instead of west to east (as was actually used). The second sequencing pattern deviated from the actual plan to mine the stope in two halves and instead simulated the mining of the stope continuously from the top to the bottom. It must be noted, however, that the results pertaining to the stress concentrations surrounding the final excavations can be somewhat misleading. EXAMINE^{TAB} requires the assumption of linear elasticity and in the case of linear elastic modelling, stress distributions around uniform geometries will be the same regardless of the intermediate steps leading up to the final geometry. Since, in most cases, the final geometry of the excavated stope will be the same, the use of the models is best applied to examining the stresses after each intermediate step. Results from the intermediate mining steps show that the actual sequencing used by the Trout Lake mine was probably the optimum pattern for keeping stresses in the sill pillar to a minimum (Fig. 12).

In the case of elasto-plastic modelling, (an option available with MULSIM/NL but not EXAMINE^{TAB}) the final stress distributions will be dependent on the sequencing since the varying zones of excavation will result in different zones of irreversible yield before the final geometry is reached. Figure. 13 shows the difference in stress concentrations for modelling the excavation with and without intermediate steps using an elasto-plastic model. The results from these two models show that without the use of intermediate mining steps, the stresses are higher towards the centre of the pillar. This would be expected since, without multiple mining steps, the amount of stress dissipation due to plastic yield would be limited. A more realistic portrayal of the resulting stress field would therefore be expected when duplicating the actual mine sequencing, since intermediate mining steps allow for large stress concentrations to gradually build up and, at the same time, slowly dissipate through plastic yielding.

Energy changes associated with mining

Another feature of the MULSIM/NL code is that it contains an energy subroutine based on work by Salamon (1984), that uses the calculated stresses and displacements at each element to determine the change in strain energy for each mining step. Strain energy is the potential energy stored in a deformed body as a result of an induced load, the derivation of which is presented in detail by Cook *et al*. (1966). Changes in strain energy accompany mining-induced stresses and result in the deterioration of the rock in the periphery of the mine opening. Energy release through rock-mass deterioration occurs violently, in the form of rockbursts, and non-violently, dissipating through the fracturing and squeezing of the near-field rock. The actual rock-mass response is defined by the mechanical properties determined from laboratory testing. The analysis of energy changes due to the sudden removal of the surrounding rock allows for an improved understanding of potential

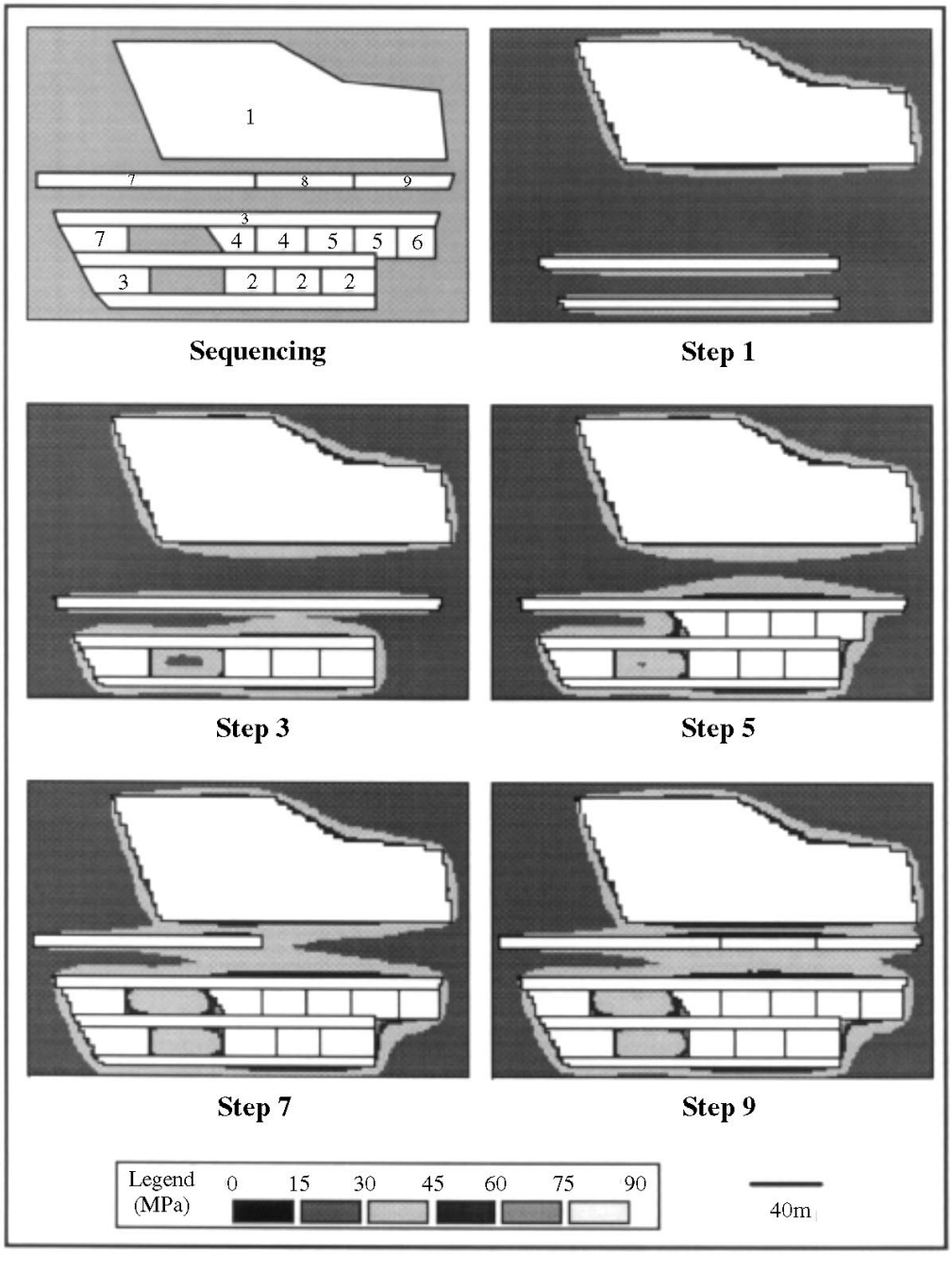

Fig. 12. EXAMINE^{TAB} excavation sequencing duplicating the actual sequencing used at the Trout Lake mine. Contours show the resulting normal stress concentrations at intermediate stages

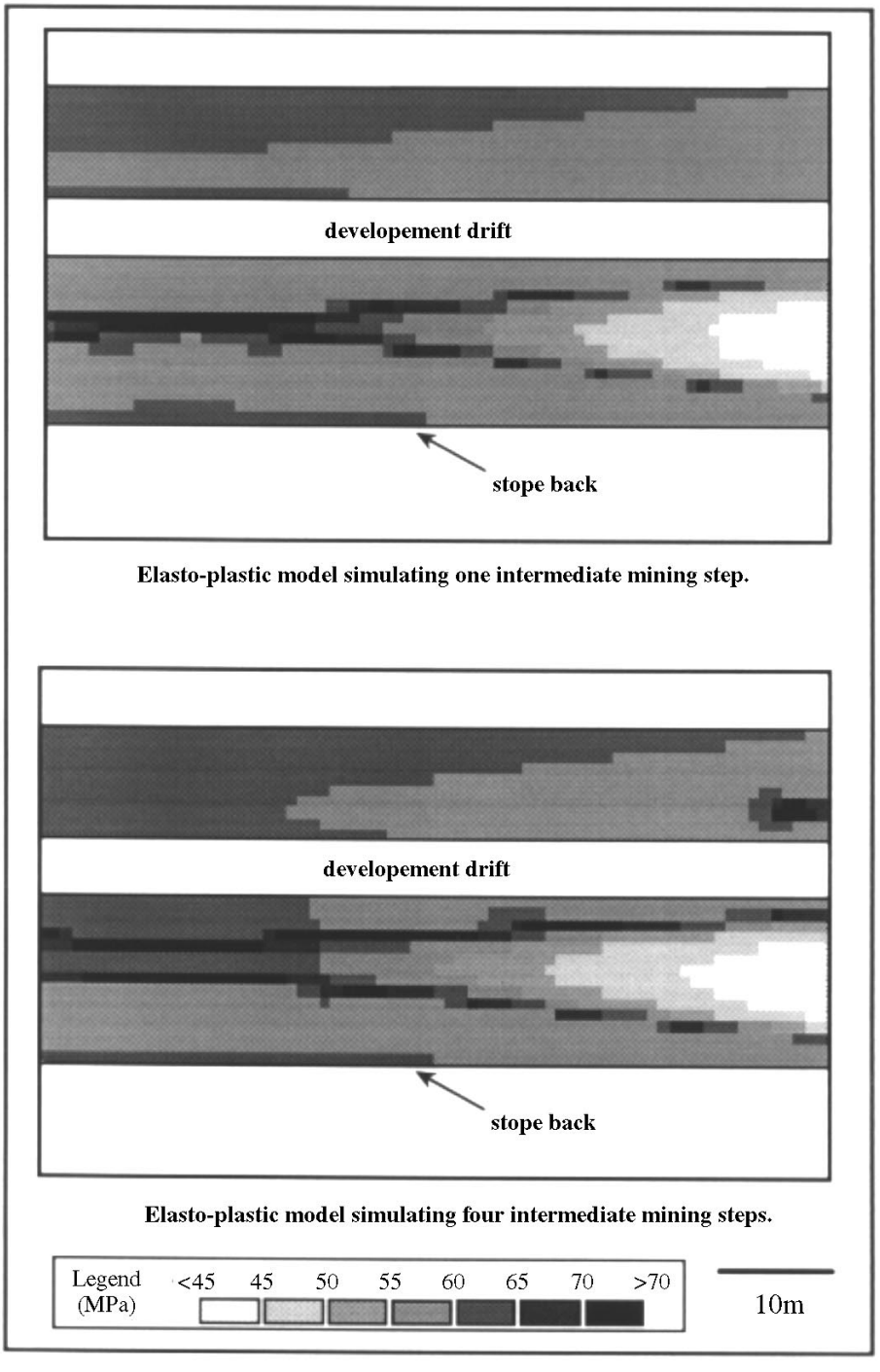

Fig. 13. MULSIM/NL elasto-plastic models demonstrating the effect of modelling the excavation as one single step or as a number of intermediate steps. Contours show the resulting normal stresses

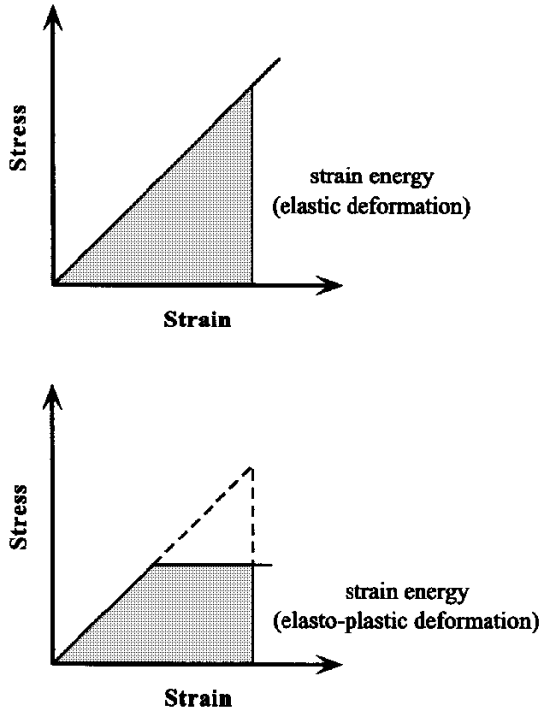

Fig. 14. Comparison of linear elastic and elasto-plastic stored strain energy using stress–strain curves

ground-control problems. In general, rock falls and other forms of violent rock failure can occur when the rate at which energy must be released as a result of mining exceeds the rate at which it can be dissipated non-violently. A study into the distribution and build-up of strain energy can provide insight not only into areas of potential instability but also into the dynamics of the potential failure.

Such a study was performed in respect to the #4 stope failure using MULSIM/NL, with comparisons being made between linear elastic and elasto-plastic models. As was expected, the influence of strain energy was seen to be more significant in the elastic model than in the elasto-plastic model, the latter model allowing for the dissipation of strain energy through plastic yielding. This principle is easily demonstrated by comparing the amount of strain energy present in an elastic medium to that present in a yielded material over the same range of strains (Fig. 14). In effect, elasto-plastic models predict a wider zone of failure, but a lower potential for violent failure, whereas linear elastic models, which do not limit the rate of strain energy build up, are more prone to indicate rock burst conditions.

Analysis of the sill pillar indicates that strain energy values in the centre of the pillar are higher for the elasto-plastic model, the opposite of what would be expected (Fig. 15). However, this can be explained by recalling that plastic yielding around the edges of the pillar results in higher stresses, and therefore strains, in the centre of the pillar. In terms of

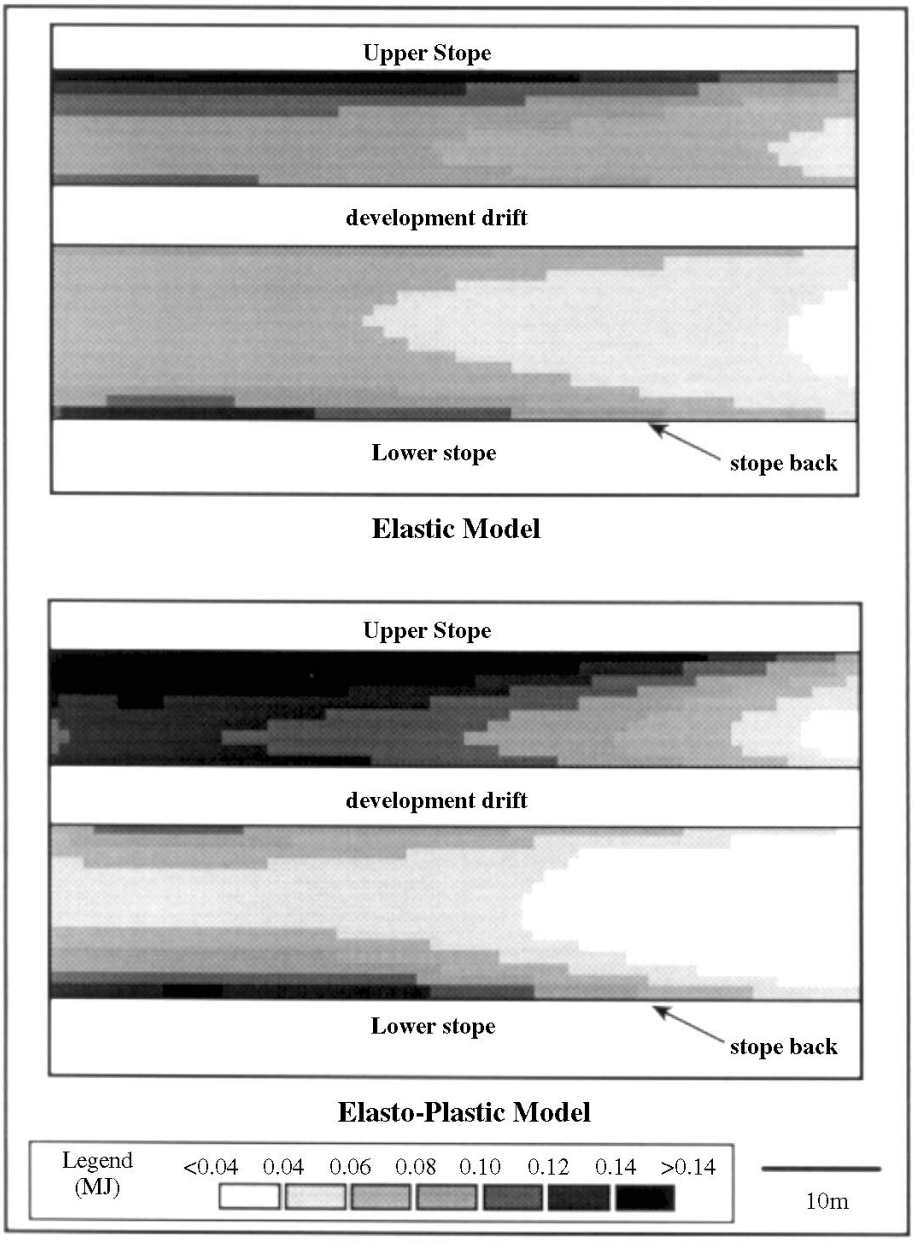

Fig. 15. Linear elastic and elasto-plastic MULSIM/NL models showing total strain energy in the sill pillar

magnitude, strain energy values in the modelled area of the failure ranged from 0.03 to 0.14 MN m/m^3 (or MJ). To clarify these results, calculations can be performed to determine the total strain energy required to cause failure in the rock. Herget (1988) notes

that in uniaxial loading conditions, if the stress reaches the failure strength of a rock, then the stored energy at failure, per unit volume, is:

$$W_o = \frac{Q_o^2}{2E} \tag{1}$$

where W_o = stored strain energy, Q_o = failure strength of the rock, and E = Young's modulus.

The simplification of uniaxial loading may be regarded as a fair assumption in this case, since stresses both near the surface of an excavation and in a support pillar are often assumed to be near uniaxial loading conditions. Performing this calculation for the disseminated ore and the solid ore using values determined through the laboratory testing, the estimated stored strain energy at failure would be approximately 0.06 and 0.16 MJ, respectively. Although this may be regarded as a crude estimate, modelling shows that the total strain energy in the failed sill pillar fell within this range. With regard to rock burst potential, Herget (1988) notes that 1.08 MJ of stored strain energy is relatively large and has the potential for bursting if suddenly released. Although failures in the #4 lens more closely conform to a gradual plastic failure, studies of strain energy build up and release rates may play a more critical role in the design of deeper stopes where the stresses are much higher.

Finite-difference method

The finite-difference and finite-element methods are both continuum codes based on the division of the problem domain into an assembly of discrete interacting nodes and elements, to which a governing set of equations are applied. These equations include the differential equations of equilibrium, the strain–displacement relationships and the stress–strain equations. Although the two methods formulate the solution of a problem in a different manner, both generate a set of linear equations that must be solved. These equations are then solved either implicitly, where the solution determines the state of stress at any time, or explicitly, where the state of stress is determined by adjacent points and time advances.

The use of the finite-difference method in geomechanical modelling is rather common, but its use in the modelling of stopes is limited. This is partly due to extensive developments in the more flexible finite-element technique overshadowing the finite-difference method (Bawden *et al*., 1988). However, developments in the method – more specifically in the commercial program FLAC (Itasca, 1992) – have provided some advantages that make it quite practical and useful for modelling. The program FLAC (Fast Lagrangian Analysis of Continua), is a 2-D, explicit finite-difference program which allows for the solution of problems involving large and non-linear deformation. Large material deformations, which can simulate yield and flow, are made possible by the use of a Lagrangian calculation scheme that is well suited for modelling large distortions and material collapse (Coetzee *et al*., 1993). In addition, the program provides several built-in constitutive models which can simulate highly non-linear, irreversible responses typical of many geological materials as well as methods of ground support.

Modelling material response for different constitutive models

The approach of solving a problem through the use of elements representing the problem domain allows the differential methods to incorporate a number of different constitutive models, representing both the anisotropy and non-linearity. These two characteristics were incorporated into the analysis of the Trout Lake mine case study. Using the 2-D finite-difference program FLAC, three models were created to compare the results of modelling the problem domain as being elastic isotropic, transversely isotropic, and Mohr–Coulomb plastic. Similar to the 2-D boundary-element programs, FLAC also uses the assumption of plane strain in the modelling of a cross-section. Meshes were constructed so that the maximum aspect ratio (element height to width) was no more than 4:1, and no more than twice the size of the element next to it in areas surrounding the stope (Fig. 16). One of the disadvantages of the finite-difference method is that special attention must be paid to the aspect ratio, since ratios greater than 5:1 can lead to significant problems with accuracy. The models were also run to simulate the excavation of the stope in three steps. This ability to follow a complete progressive stoping operation was commented on by Hart (1980), as showing the wide versatility of the finite-difference method.

The FLAC results for the three different material models showed similar results, with stress concentrations in the sill pillar varying by only a few MPas (Table 4). Even with reductions in the property values to reflect the minimum standard deviation of the laboratory test results, stress values in the sill pillar stayed consistent. Although the finite-difference method uses the elastic properties in the calculation of the stresses through a relaxation method, the magnitude of the differences between the three models was insignificant. This is as expected since for linear elastic problems, the material properties affect only the strains, not the stresses. In addition, results from these models basically show the same results as those obtained through the other numerical methods. In general, large stress shadows of the order of magnitude of approximately 50 MPa appear around the ends of the stopes with larger concentrations occurring in the sill pillar where the actual stope failure began. Similar to the elasto-plastic displacement-discontinuity models, the FLAC elasto-plastic model showed lower stresses than the elastic models (indicating destressing of the rock through yield) and a more widespread influence of stress concentrations. The similarities found between the linear elastic and transversely isotropic models, and the results obtained through the simpler and less time-consuming elastic integral method models, demonstrates the relative inefficiency of the finite-difference method in elastic modelling of homogeneous media. It is the ability of the differential method to model materials as being plastic or non-linear, along with the handling of anisotropy and inhomogeneity, that separates it from the integral method in terms of practical use.

Modelling plastic yield and failure mechanisms

A study into the failure mechanisms responsible for the #4 stope failure was performed through the use of the Mohr–Coulomb elasto-plastic constitutive model. Exploiting FLAC's use of the Mohr–Coulomb material model, the stress magnitudes can be compared to this failure criterion to determine the state of yield in the rock mass. Comparisons between the yielded rock and the stress trajectories provides considerable insight into the

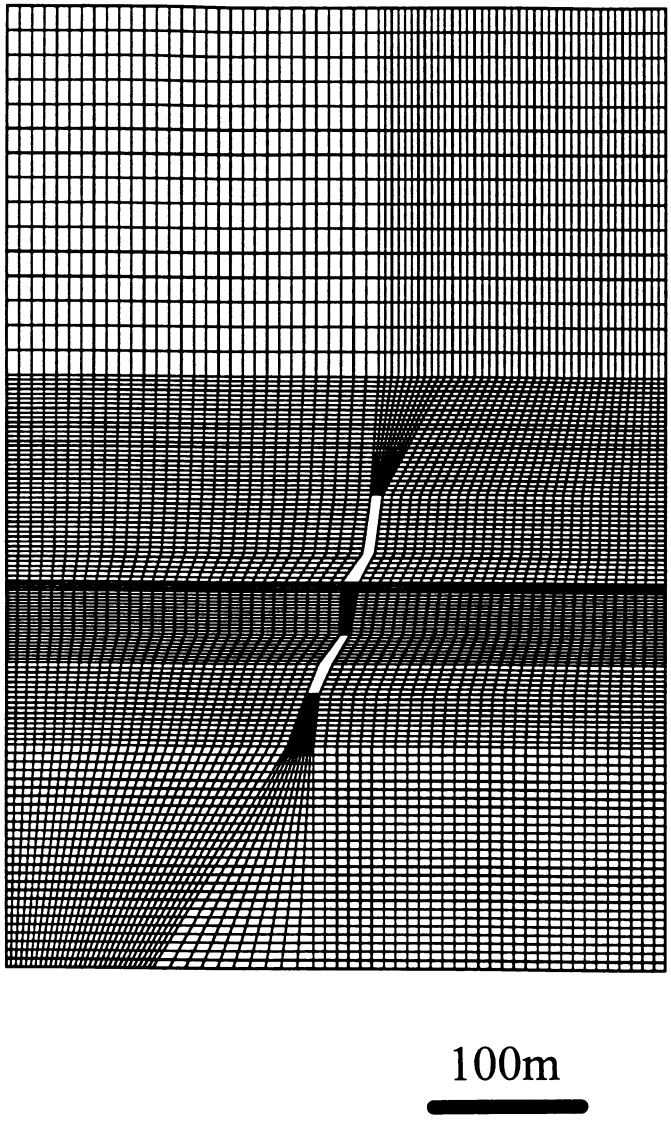

Fig. 16. FLAC mesh for the 500E cross-section

failure mechanism responsible for the #4 lens failure. Results from the modelling indicated that, with the weaker strength properties of the disseminated ore, yield would be initiated in the disseminated ore (Fig. 17a). Assuming that this yield would result in compressive failure of the disseminated ore and therefore its subsequent unravelling, the yielded blocks were removed from the model. Subsequent modelling runs show that the unravelling of the disseminated ore results in a rotation of the stress field around the stope. This results in higher compressive stresses in the disseminated ore, and unconfined to tensile stresses in the solid ore next to it (Fig. 17b). It should be noted that the modelling results correlated

Table 4. Predicted maximum principal sill-pillar stress magnitudes using FLAC analyses and various assumed constitutive models

Material model	Maximum principal stress in sill pillar (MPa)		
	2m above opening	10m above opening	20m above opening
Linear elastic (average lab values)	54.5	30.1	29.2
Transversely isotropic (average lab values)	53.6	30.3	29.3
Mohr–Coulomb plastic (average lab values)	52.3	31.0	29.9
Linear elastic (minimum lab values)	56.5	29.3	28.5
Mohr–Coulomb plastic (minimum lab values)	48.6	32.2	30.8

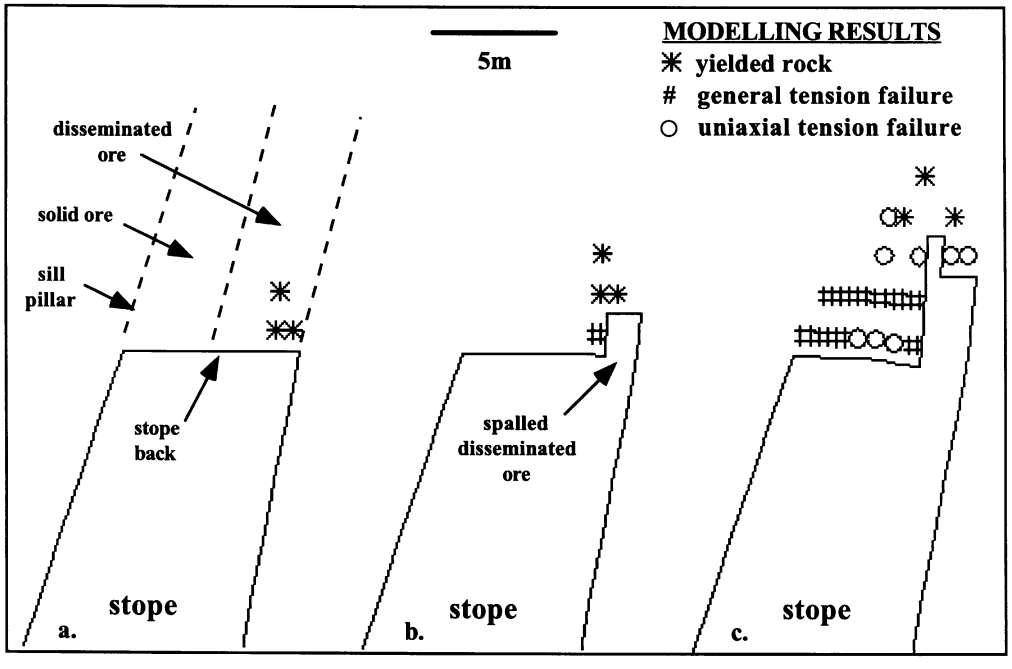

Fig. 17. FLAC plots showing (a) state of yield in the rock within the sill pillar above the lower half of the excavated stope, (b) the resulting state of yield in the orebody after the removal of the yielded blocks, (c) further state of yield after the continued removal of yielded disseminated ore blocks, resulting in large scale failure of the sill pillar. At yield indicates that the rock has surpassed its yield point in the failure criterion

well to underground observations of the failure; unravelling of the disseminated ore was initially reported prior to the eventual large-scale failure of the stope back.

Further modelling shows that the removal of only a few cubic metres of disseminated ore through small scale compressive failures results in the further yielding of the disseminated ore. Repeating the process of removing the yielded disseminated ore

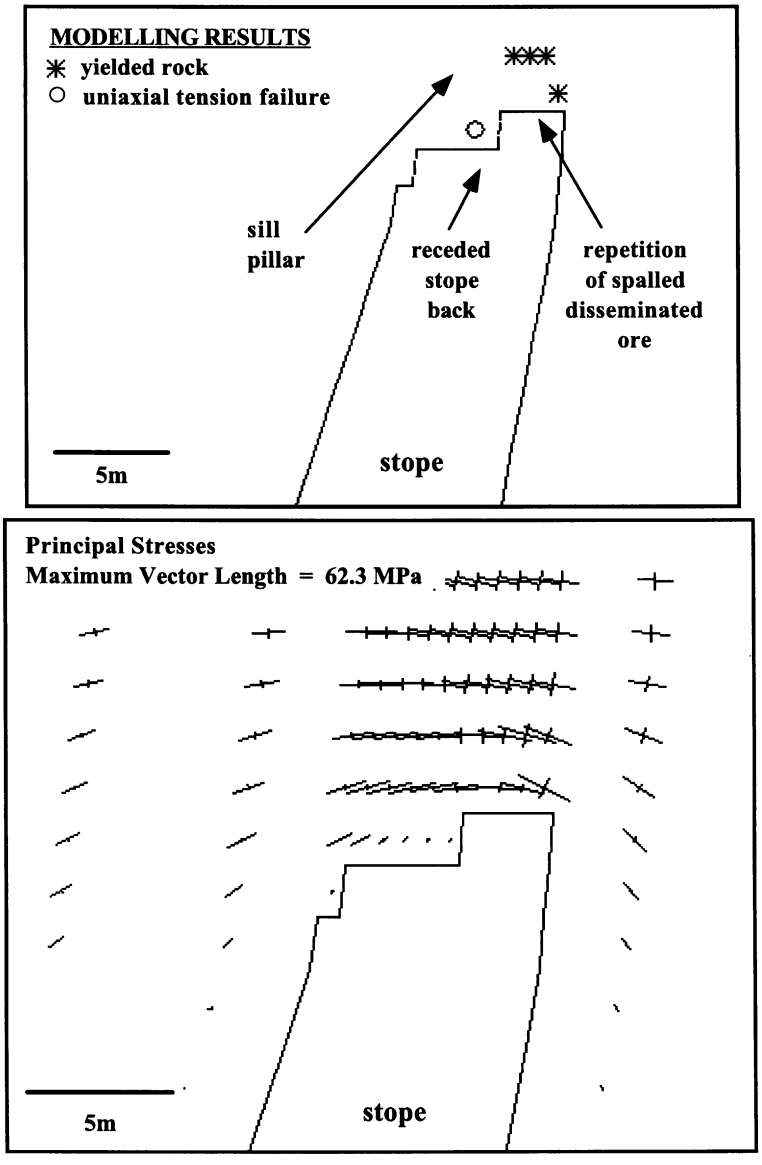

Fig. 18. FLAC results showing the repetition of the failure cycle after large scale failure with small yield zones in the disseminated ore

eventually results in a 'chimneying' effect where the propagation of failure in the disseminated ore leads to a loss of confinement of the solid ore back. The model shows that with this 'chimney' along the footwall, tensile failure occurs in the solid sulphide rock mass (Fig. 17c). Underground, this is seen as fracturing of the back and large-scale wedge failures. Subsequent models show that the large-scale failure of the solid sulphide rock mass allows the stresses to reach an apparent equilibrium. The cycle then begins again

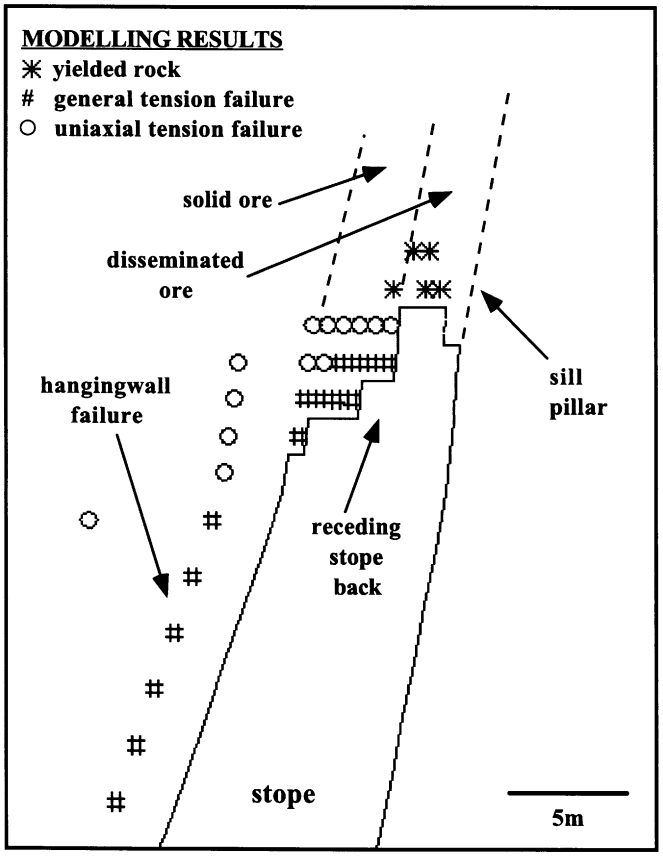

Fig. 19. FLAC results showing the eventual failure of the hanging wall with continued failure in the ore zone

with small scale unravelling in the disseminated ore due to compressive failure and large-scale wedge failure of the solid sulphide rock mass (Fig. 18). Modelling also shows that with the continuing failure of the sill pillar and the rotation of the stress field around the stope, destressing occurs in the hanging wall. This is likely to result in stability problems in the relatively stronger hangingwall (Fig. 19).

Conclusion

A design methodology applicable to steeply dipping orebodies typical of many underground hardrock mines has been presented. This methodology was developed through a study on the #4 lens stope failure at the Trout Lake mine of the Hudson Bay Mining and Smelting Co., Ltd, Flin Flon, Manitoba, using elements of laboratory testing, rock-mass characterization and computer modelling. The objective of the case study was to investigate the mechanisms responsible for the failure, with the possible adoption of the

design methodology to prevent similar failures at increased mining depths and consequently higher induced stresses.

Laboratory testing and rock-mass characterization formed the first stage of this investigation. Results from this study provided information on the constitutive behaviour and in determining failure strength criteria for the four rock types encountered in the study area. A more thorough understanding of the rock-mass behaviour was obtained through the analysis of *in situ* behaviour in the form of an empirical design methodology, more specifically Mathews' stability graph method. This analysis was augmented by observations made in the mine pertaining to the failed stope. The results of the laboratory and *in situ* analysis were then used in the second, or design stage, of the investigation.

The design stage involved the evaluation of selected numerical modelling techniques in the investigation of ground performance in the near-field rock surrounding an excavated stope. An approach was developed whereby several numerical methods could be used in conjunction, allowing for the advantages of each method to be maximized, providing a comprehensive analysis from different perspectives of stope design. This methodology deviates from approaches more commonly cited in the literature where the use of only one or two programs, capable of performing a limited set of tasks, is investigated. The methodology includes the use of:

1. boundary-element techniques to investigate 2-D and 3-D geometry related stress concentrations. By utilizing the speed and efficiency of the boundary-element method, a large number of geometries may be analysed in a relatively short period of time;
2. displacement-discontinuity techniques to study pseudo 3-D elasto-plastic deformations, mine sequencing and strain energy build-up. The method is suitable for analysing open stope geometries, providing further detailed analysis than that allowed by the boundary-element method;
3. differential techniques (finite-difference, finite-element) to model non-linear, anisotropic behaviour. The flexibility of the method proves a useful tool in the study of yield zones and ground failure mechanisms.

To date, a 3-D differential analysis has not been included in this methodology. By utilizing the differential methods' ability to include the constitutive model of different materials, a more realistic portrayal of the problem might be obtained using a 3-D non-linear finite-element or finite-difference code. Although this type of analysis provides a more realistic representation of the problem, it is also more complex and time consuming. In addition, more input data is required, more assumptions may need to be made, and the use of instrumentation data to constrain the model becomes still more critical. With the eventual development of more powerful computers and more user friendly software, the inclusion of 3-D finite-element and finite-difference analysis will become more accessible and routine as a design tool.

References

Anon. (1985) Suggested method for determining point load strength. *International Journal of Rock Mechanics and Mining Sciences & Geomechanical Abstracts*, **22**(2), 51–60.

Barla, G. and Innaurato, N. (1973) Indirect tensile testing of anisotropic rocks. *Rock Mechanics*, **5**, 215–30.

Barton, N. (1990) Scale effects or sampling bias? in *Scale Effects in Rock Mechanics*, A. Pinto da Cunha, (ed.), A.A. Balkema, Norway, pp. 31–55.

Barton, N., Lien, R. and Lunde, J. (1974) Engineering classification of rock masses for the design of tunnel support. *Rock Mechanics*, **6**, 189–236.

Bawden, W.F. and Milne, D. (1987) Geomechanical mine design approach at Noranda Minerals Inc., in *Proceedings of the 6th ISRM International Congress on Rock Mechanics*, Herget, G. and Vongpaisal, S. (eds), Montreal, A.A. Balkema, Rotterdam, pp. 799–803.

Bawden, W.F., Milne, D.M., Hrastovich, W., Germain, P. and Kanduth, H. (1988). Computer applications in geomechanical stope and pillar design at Noranda Minerals Inc., *Proceedings of the 1st Canadian Conference on Computer Applications in the Mineral Industry*, Fytas, K., Collins J.L.,and Singhal, R. (eds), Québec, A.A. Balkema, Rotterdam, pp. 291–8.

Bawden, W., Sauriol, G., Milne, D. and Germain, P. (1989) Practical rock engineering stope design case histories from Noranda Minerals Inc., *CIM Bulletin*, **82** (927), 37–45.

Beer, G. (1988) Application of 3-D boundary element and coupled analysis in geomechanics: case studies, in *Proceedings of the 6th International Conference on Numerical Methods in Geomechanics*, Swoboda, G. (ed.), Innsbruck, A.A. Balkema, Rotterdam, pp. 2209–16.

Brady, B.H. (1977) An analysis of rock behaviour in an experimental stoping block at the Mount Isa Mine, Queensland, Australia. *International Journal of Rock Mechanics and Mining Sciences & Geomechanical Abstracts*, **14**(2), 59–66.

Brady, B.H. and Brown, E.T. (1993) *Rock Mechanics for Underground Mining*, Chapman & Hall, New York.

Brady, T.M. and Johnson, J.C. (1989) Comparison of a finite-difference code to a finite-element code in modelling an excavation in an underground shaft pillar, in *Proceedings of the 3rd International Symposium on Numerical Modelling in Geomechanics (NUMOG III)*, S. Pietruszczak and G.N. Pande (eds), Niagara Falls, Elsevier Applied Science, London, pp. 608–19.

Brummer, R.K. (1985) A simplified modelling strategy for describing rock mass behaviour around stope faces in deep hard-rock gold mines, in *Proceedings of the 26th U.S. Symposium on Rock Mechanics: Research and Engineering Applications in Rock Masses*, Ashworth, E. (ed.), Rapid City, S. Dakota, A.A. Balkema, Rotterdam, pp. 113–20.

Coetzee, M.J., Hart, R.D., Varona, P.M. and Cundall, P.A. (1993) *FLAC Basics: An Introduction to FLAC and a Guide to its Practical Application in Geotechnical Engineering*, Itasca Consulting Group Inc., Minneapolis.

Cook, N.G.W., Hoek, E., Pretorius, J.P.G., Ortlepp, W.D. and Salamon, M.D.G. (1966) Rock mechanics applied to the study of rockbursts. *Journal of the South African Institute of Mining and Metallurgy*, **66**(10), 435–528.

Crouch, S.L. and Starfield, A.M. (1983) *Boundary Element Methods in Solid Mechanics: With Applications in Rock Mechanics and Geological Engineering*, George Allen & Unwin, London.

Cundall, P.A. (1971) A computer model for simulating progressive large scale movements in blocky rock systems, in *Rock Fracture, Proceedings of the International Symposium on Rock Mechanics*, Nancy, p. II-8.

Curran, J.H. and Corkum, B.T. (1988) *EXAMINE^{2D} Version 3.1 Users Manual: a 2D Boundary Element Program for Calculating Stresses Around Underground Excavation in Rock*, Data Visualization Laboratory, Department of Civil Engineering, University of Toronto.

Curran, J.H. and Corkum, B.T. (1993) *EXAMINE^{3D} Version 2.0 Users Manual: Three-dimensional Excavation Analysis for Mines*, Data Visualization Laboratory, Department of Civil Engineering, University of Toronto.

Curran, J.H., Corkum, B.T. and Wyllie, J.A. (1990) *EXAMINE^{TAB} Version 1.1 Users Manual: Excavation Analysis for Mines*, Data Visualization Laboratory, Department of Civil Engineering, University of Toronto.

Eberhardt, E., Stead, D. and Szczepanik, Z. (1994) *Characterization of Rock Masses Within the Flin Flon Mining Area*, Hudson Bay Mining and Smelting Co., Ltd, Grant-in-Aid Report.

Franklin, J.M., Lydon, J.W. and Sangster, D.F. (1981) Volcanic-associated massive sulphide deposits, *Economic Geology* 75th Anniversary Volume, Skinner, B.J. (ed.), Economic Geology Publishing Co., El Paso, Texas, pp. 485–627.

Grant, D.R., Potvin, Y. and Rocque, P. (1993) Three dimensional stress analysis techniques applied to mine design at Golden Giant Mine, in *1st Canadian Symposium on Numerical Modelling Applications in Mining and Geomechanics*, Mitri, H.S. (ed.), Montreal, McGill University, Montreal, pp. 5–16.

Hart, R.D. (1980) Geotechnical modelling of a cut and fill mining operation, in *Proceedings of the Conference on the Application of Rock Mechanics to Cut and Fill Mining*, Stephansson, O. and Jones, M.J. (eds), Lulea, Sweden, Institute of Mining and Metallurgy, London, pp. 307–15.

Herget, G. (1988) *Stresses in Rock*, A.A. Balkema, Rotterdam.

Hoek, E., Grabinsky, M.W. and Diederichs, M.S. (1991) Numerical modelling for underground excavation design. *Transactions of the Institution of Mining and Metallurgy (Section A: Mining Industry)*, **100**, A22–A30.

Itasca Consulting Group, Inc. (1992) *FLAC Version 3.22*, Itasca Consulting Group Inc., Minneapolis.

Ko, C.B. (1986) *Geology of the Trout Lake Copper–Zinc Sulphide Deposit*, Hudson Bay Mining and Smelting Co., Ltd, Internal Report.

Kwasniewski, M. (1983) Anisotropy of elasticity of rocks and its effect on the magnitude and distribution of stresses around underground openings, in *Proceedings of the 8th Plenary Scientific Session of the International Bureau of Strata Mechanics: Application of Rock Mechanics to Planning and Design Prior to Mining*, A. Kidybinski and M. Kwasniewski (eds), Essen, Germany, A.A. Balkema, Rotterdam, pp. 5–37.

Laubscher, D.H. and Taylor, H.W. (1976) The importance of geomechanics classification of jointed rock masses in mining operations, in *Proceedings of the Symposium on Exploration for Rock Engineering*, Bieniawski, Z.T. (ed.), A.A. Balkema, Cape Town, Johannesburg, Vol. 1, pp. 119–128.

Martin, C.D. (1993) The strength of massive Lac du Bonnet granite around underground openings, PhD thesis, Department of Civil Engineering, University of Manitoba, Winnipeg, MB.

Mathews, K.E., Hoek, E., Wyllie, D.C. and Stewart, S.B.V. (1980) *Prediction of Stable Excavations for Mining at Depths Below 1000 Metres in Hard Rock*, CANMET Report 802–1571 (Serial No. OSQ80-00081).

Niemi, W.R., Page, C., Moss, A. and Yu, Y. (1987) Applied rock mechanics at Thompson mine: a study in practicality, in *13th World Mining Congress: Improvement of Mine Productivity and Overall Economy by Modern Technology*, Almgren, G., Berge Z. and Matikainen R. (eds), Stockholm, A.A. Balkema, Rotterdam, pp. 167–76.

Pakalnis, R.C., Miller, H.D., Vongpaisal, S. and Madill, T. (1987) An empirical approach to open stope design, in *Proceedings of the 6th ISRM International Congress on Rock Mechanics*, Herget, G. and Vongpaisal, S. (eds), Montreal, A.A. Balkema, Rotterdam, pp. 1191–6.

Pakalnis, R., Tenney, D. and Lang, B. (1991) Numerical modelling as a tool in stope design. *CIM Bulletin*, **84** (951), 64–73.

Pande, G.N., Beer, G. and Williams, J.R. (1990) *Numerical Methods in Rock Mechanics*, John Wiley & Sons, Toronto.

Pariseau, W.G. and Duan, F. (1987) A three dimensional finite element analysis of the VCR study stope at the Homestake mine, in *Proceedings, Fifth Annual Workshop, Generic Mineral Technology Center, Mine Systems Design and Ground Control*, Topuz, E. and Lucas, J.R.

(eds), Tuscaloosa, Alabama, Virginia Polytechnic Institute and State University, Virginia, pp. 67–78.

Pinto, J.L. (1970) Deformability of schistose rocks, in *Proceedings of the 2nd ISRM International Congress on Rock Mechanics*, Belgrade, pp. 491–6.

Read, S.A.L., Perrin, N.D. and Brown, I.R. (1987) Measurement and analysis of laboratory strength and deformability characteristics of schistose rock, in *Proceedings of the 6th ISRM International Congress on Rock Mechanics*, Herget, G. and Vongpaisal, S. (eds), Montreal, A.A. Balkema, Rotterdam, pp. 233–8.

Reschke, A.E. and Romanowski, J. (1993) The success and limitations of Mathews analysis for open stope design at HBMS, Flin Flon operations, *95th CIM Annual General Meeting*, Calgary, Paper 136.

Salamon, M.D.G. (1984) Energy considerations in rock mechanics: fundamental results, *Journal of the South African Institute of Mining and Metallurgy*, **84**(8), 233–246.

Spottiswoode, S.M. (1990) Towards 3-D modelling of inelastic deformation around deep-level mines, in *Proceedings of the International Conference on Mechanics of Jointed and Faulted Rock*, Rossmanith, H.P. (ed.), Vienna, A.A. Balkema, Rotterdam, pp. 695–707.

Tsidzi, K.E.N. (1990) The influence of foliation on point load strength anisotropy of foliated rocks, *Engineering Geology* **29**, 49–58.

Wagner, H. (1980) Pillar design in coal mines, *Journal of the South African Institute of Mining and Metallurgy*, **80**, 37–45.

Zipf, R.K. (1992a) *MULSIM/NL Theoretical and Programmer's Manual*, US Bureau of Mines, Information Circular 9321.

Zipf, R.K. (1992b) *MULSIM/NL Application and Practitioner's Manual*, US Bureau of Mines, Information Circular 9322.